water

MDPI

Article

Reliable Future Climatic Projections for Sustainable Hydro-Meteorological Assessments in the Western Lake Erie Basin

Sushant Mehan [1,*], Margaret W. Gitau [2,*] and Dennis C. Flanagan [3]

[1] Water Resources Engineer, Sacramento, CA 95931, USA
[2] Department of Agricultural and Biological Engineering, Purdue University, West Lafayette, IN 47907, USA
[3] USDA-Agricultural Research Service, National Soil Erosion Research Laboratory, 1196 Building SOIL, Purdue University, 275 S. Russell Street, West Lafayette, IN 47907-2077, USA; flanagan@purdue.edu
* Correspondence: sushantmehan@gmail.com (S.M.); mgitau@purdue.edu (M.W.G.)

Received: 28 February 2019; Accepted: 16 March 2019; Published: 20 March 2019

Abstract: Modeling efforts to simulate hydrologic processes under different climate conditions rely on accurate input data. Among other inaccuracies, errors in climate projections can lead to incorrect decisions. This study aimed to develop a reliable climate (precipitation and temperature) database for the Western Lake Erie Basin for the 21st century. Two statistically downscaled bias-corrected sources of climate projections (GDO: Global Downscaled Climate and Hydrology Projections and MACA: Multivariate Adaptive Constructed Analogs) were tested for their effectiveness in simulating historic climate (1966–2005) using ground-based station data from the National Climatic Data Center. MACA was found to have less bias than GDO and was better at simulating selected climate indices; thus, its climate projections were subsequently tested with different bias correction methods including the power transformation method, variance scaling of temperature, and Stochastic Weather Generators. The power transformation method outperformed the other methods and was used in bias corrections for 2006 to 2099. From the analysis, mean daily precipitation values were expected to remain more or less the same under both RCP (Representative Concentration Pathway) 4.5 and RCP 8.5 scenarios, ranging between 2.4 mm and 3.2 mm, while standard deviations were expected to increase, pointing to a rescaling of the distribution. Maximum one-day precipitation was expected to increase and could vary between 120 and 650 mm across the basin, while the number of wet days could potentially increase under the effects of RCP 4.5 and RCP 8.5. Both mean maximum and mean minimum daily air temperatures were expected to increase by up to 5.0 °C across the basin, while absolute maximum and minimum values could increase by more than 10 °C. The number of days in which precipitation could potentially fall as snow was expected to decrease, as was the annual number of days for optimal corn growth, although an earlier start to the growing season could be expected. Results from this study were very useful in creating a reliable climate database for the entire Western Lake Erie Basin (WLEB), which can be used for hydrologic, water resources, and other applications in the basin. The resulting climate database is published and accessible through the Purdue University Research Repository (Mehan et al., 2019), which is an open-access repository.

Keywords: climate projections; Western Lake Erie Basin; bias correction; water resources; open access

1. Introduction

Predictive hydrologic studies require accurate weather input to simulate hydrologic processes within a watershed [1]. Any inaccuracies or bias associated with the weather data may lead to deleterious effects on simulated outputs [1–3]. As a rule of thumb, the better the input climate data, the more reliable the outcomes of modeling studies can be. Transport of pollutants as well as their dilution by water flows are also dependent upon climate [4]. Moreover, studies based on impacts on hydrological processes due to changing climate have become possible using results from simulations from large-scale general climate models. However, climate projections at regional scales suffer from some bias because of the influence of local factors [5–7]. These local factors include topography and catchment characteristics, atmospheric circulation, and moisture supply [8,9], and usually produce errors or bias within climate values, which may alter the outputs of many different model application studies.

For the U.S. Great Lakes Region, and in particular for the Western Lake Erie Basin (WLEB), data for several Representative Concentration Pathways (RCPs) (RCP 2.6, RCP 4.5, RCP 6, RCP 8.5) scenarios from different GCM (General Circulation Model) models at varied resolutions (100 km–600 km) are available [10–12]. For this study, WLEB is an area of interest because phosphorus loadings from agricultural lands within the basin are the major cause of harmful and nuisance algae blooms (HNAB) in Lake Erie. To facilitate policy planning and mitigation measures to control this nuisance, it is very important to assess nutrient loadings in future climatic conditions. Due to their coarse resolution and large uncertainties associated with downscaling [13], it is a challenge to use available GCM outputs within WLEB for hydrologic studies. These coarser resolution products from GCMs need to be resolved into finer resolution Regional Climate Models (RCMs), which is achieved using different downscaling techniques (statistical and dynamic), which are discussed in greater detail in subsequent paragraphs.

In statistical downscaling, the relationship between large-scale climate variables from GCMs (predictors) is determined using fine-scale climate variables for RCM [7]. Statistical downscaling is computationally inexpensive, requires less time, and involves different methods to produce the projections [7]. On the other hand, dynamic downscaling techniques develop an RCM that is derived from a GCM with the same set of empirical equations and physical principles that were used to develop the GCM [5,14]. The outputs are resolved at a resolution less than 50 km and can be used for regional studies at the catchment scale [13,15]. A major limitation with simulated outputs from dynamic downscaling is that the resulting RCM may not be applicable to locations other than the region for which it was developed [16]. Some errors associated with baseline climate data [17] and many of the natural variabilities and uncertainties, including future greenhouse gas emissions, the structure of climate models and their parameterization, and downscaling techniques [18], can make it difficult to obtain sufficient or viable model runs based on computations and resource availability, which may produce some biases [15]. Thus, in either downscaling approach, there may be the need for post-processing of the projected output from a downscaled GCM [19] to correct for bias in the data.

Bias correction and perturbation are post-processing options for data following downscaling [20]. Bias correction helps to maintain the statistical relationships between the distributions of observations and model outputs of different climate variables for the current period simulated along with future periods [20]. The perturbation approach assumes that change in the distribution of observations from current to future will be the same as the model distribution [21].

Different bias correction techniques can lead to different results in climate change impact studies [15,22]. Therefore, it is very important to quantify the bias in outputs generated from the climate models before they are applied in climate change impact modeling studies [15]. Different sources of uncertainty arising from GCM or RCM structure and hydrological model parameterization have been studied but evaluation of GCM and RCM model outputs of different climate variables for climate change impact studies are rarely studied [23]. Previous climate change implication studies in the WLEB have used projected daily climate data summaries from different sources without quantifying the associated bias [24–26]. This study addresses the gap where reliable climate information for simulating future water resource responses in the WLEB is lacking. The goal was to develop a framework to evaluate and correct biases associated with simulated climate output from the most reliable and easy to access statistical downscaled models available in the public domain for the WLEB and produce a reliable climate database for the entire WLEB for the period 2006–2099.

This manuscript comprises three major research objectives, to: (1) assess two sources of climate projections available in the public domain and, based on bias quantification, select the one having less bias for further analysis; (2) evaluate the performance of different methods in correcting the bias of the climate values for the historical period (1966–2005); and, (3) develop future climate values for the 21st century for the WLEB using the most effective bias correction method.

2. Materials and Methods

2.1. Study Site and Climatology

The 29,137 km^2 Western Lake Erie Basin (WLEB) extends across portions of Michigan, Indiana, and Ohio, and drains into Lake Erie, the shallowest of the five U.S. Great Lakes (Figure 1). For this study, eight stations, as shown in Figure 1, were selected for analysis based on data availability (>95%) and consistency, and to provide spatial coverage across the basin. Based on data from these selected stations, the total annual precipitation varied from 1050 mm to 1200 mm (1966–2005). More precipitation occurred during the spring season. To answer the research questions in this study, three of the eight stations (Adrian, MI, Fort Wayne, IN, and Norwalk, OH) were used for methodology development, approaches from which were then extended to the other five stations. The three stations were selected based on [27] with considerations including geographical location and differences in precipitation. Of the three stations, Norwalk, OH had the highest one-day maximum precipitation based on daily precipitation records for this period (Figure 2A). Precipitation at this station also occurred more frequently and over longer periods than with the other two stations. The temporal spread of precipitation varied and with the diverse geographic coverage, these three stations were considered satisfactory to answer the first two major questions of this study.

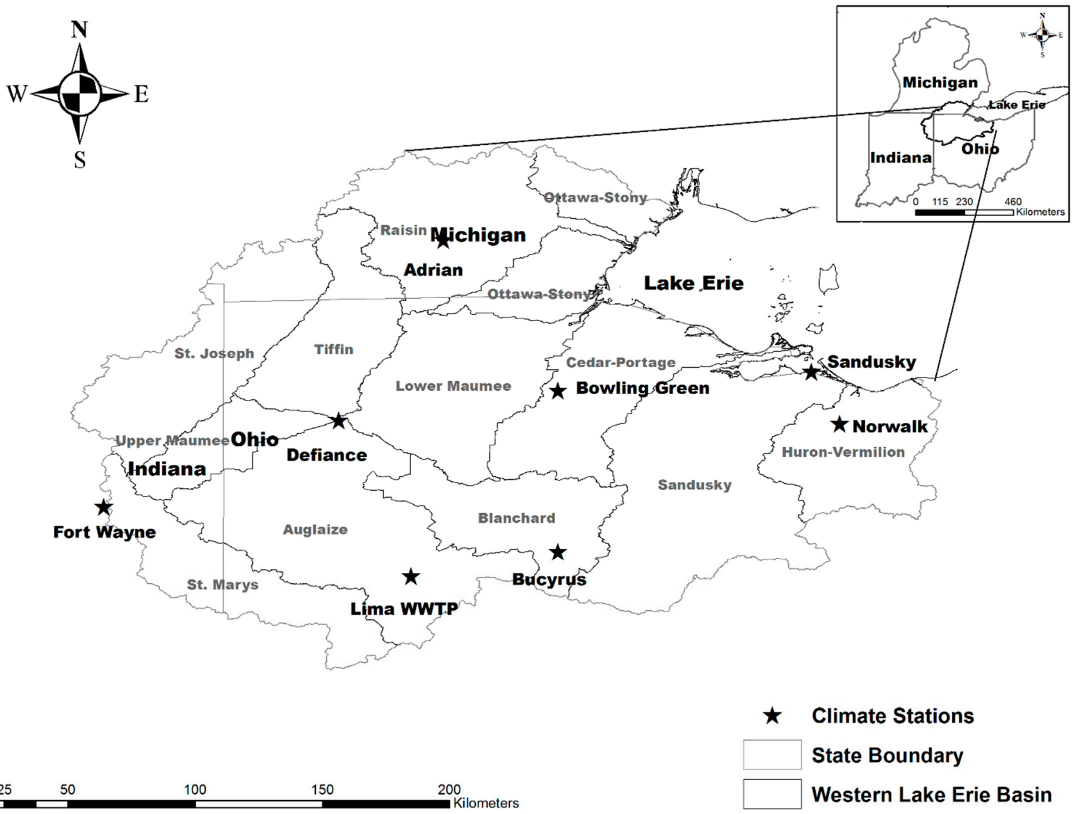

Figure 1. Pilot site: The Western Lake Erie Basin (WLEB) and different ground-based climate stations considered in this study.

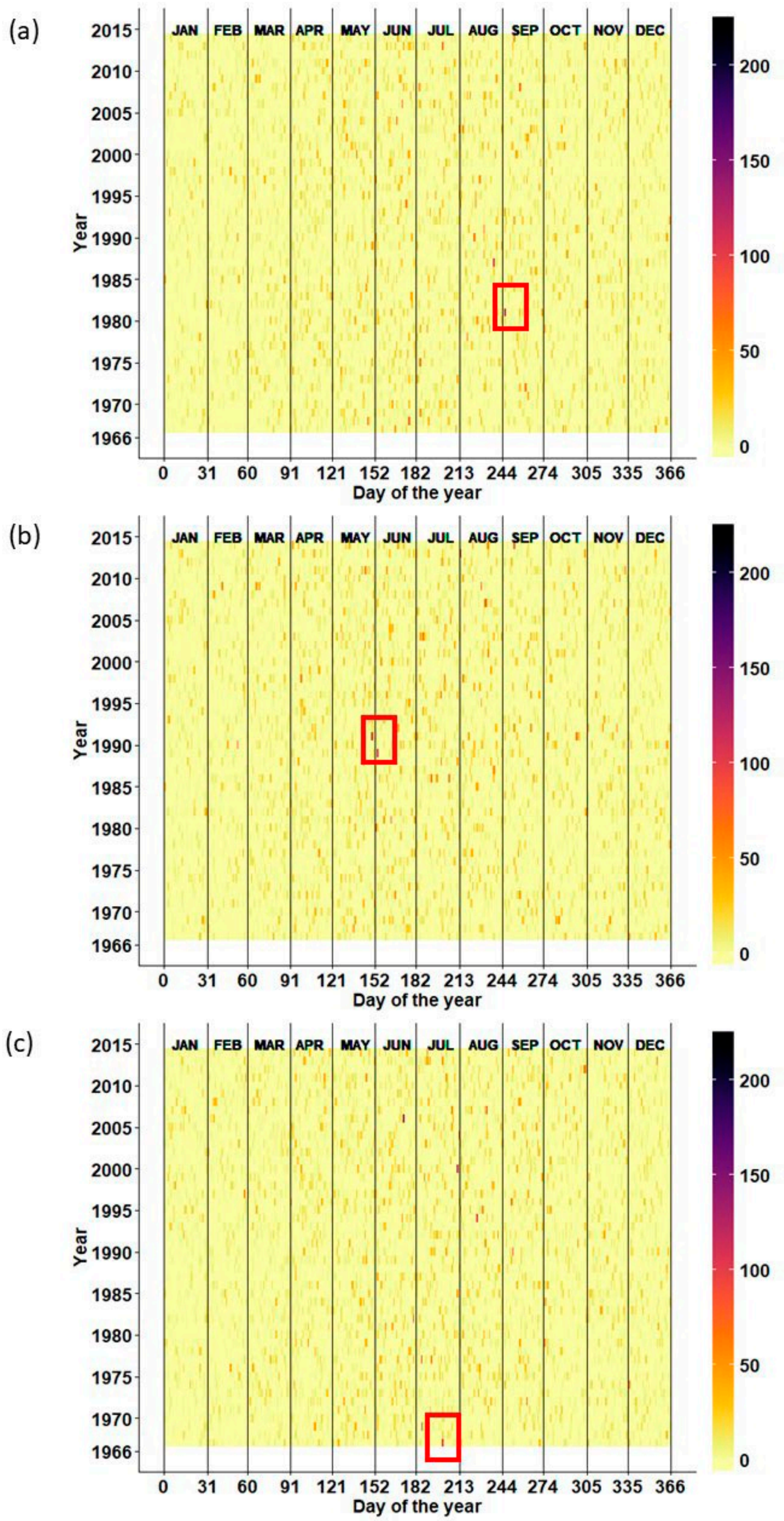

(**A**)

Figure 2. *Cont.*

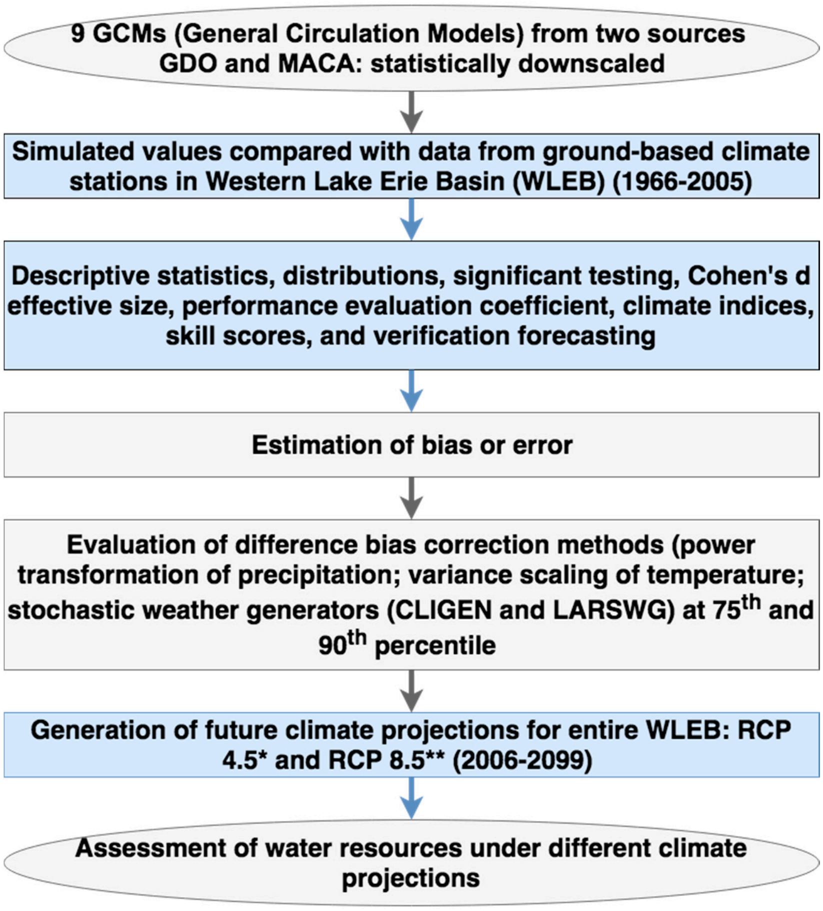

(**B**)

Figure 2. (**A**) Temporal distribution of daily precipitation records (mm), for (**a**) Adrian, MI; (**b**) Fort Wayne, IN, and (**c**) Norwalk, OH from 1966 to 2015 from the respective ground-based weather stations. Red boxes show the greatest magnitude precipitation event for each station. (**B**) Executive summary of the methodology. *; **: RCP: Representative Concentration Pathways (Radiative forcing); Currently: 300–400 ppm; RCP 4.5: 4.5 W/m^2; RCP 8.5: 8.5 W/m^2.

2.2. Data Acquisition

Downscaled climate data for this project were obtained from two sources: (1) GDO (authors created acronym for Global Downscaled Climate and Hydrology Projections), available at https://gdo-dcp.ucllnl.org/downscaled_cmip_projections/; and (2) MACA (Multivariate Adaptive Constructed Analogs), available at https://climate.northwestknowledge.net/MACA/. The historical period for both sources was 1950–2005 and future climate projections were for 2006–2099. Data from both sources were statistically downscaled from the set of GCMs and have been used in previous climate change studies [24,28,29]. The sources provide fine spatial resolution translations of climate projections over the United States based on the multi-model dataset referenced in the IPCC AR 5 (CMIP5) to an extent of 0.25 and 0.04 degrees, sufficient for regional climate impact assessment studies [30].

The GDO source incorporates non-dynamic approaches including monthly Bias correction and Spatial Disaggregation (BCSD) and daily Bias-corrected and Constructed Analogue (BCCA), which have been well tested and automated to produce output statistics matching those of a historical period for fine-scaled gridded precipitation and temperature [30]. Under the BCSD method, quantiles of historical patterns are related to quantiles of predictions from the GCM to project daily time series for the downscaled grid. GCM predictions are matched statistically with a set of observed historical weather patterns to develop the fine-scale map while downscaling using the BCCA method. The drawback of using GDO downscaled data is the assumption that the statistical properties of the high-resolution GCM and local-scaled RCM after downscaling, including mean and variance are constant through time, which is not necessarily the case [31,32].

In the MACA source both the observation dataset and GCM outputs are resolved to either 4 km or 6 km. To overcome the problem of limited availability of suitable weather analogues in a changing climate, seasonal and annual trends at each grid point are computed using 21 days, 31-year running mean of data. A cumulative distribution function (CDF) of 15 days is computed at each grid point using non-parametric quantile mapping, and the CDF of historical data is used for bias correction. The final outputs are consistent with the GCM data and compatibility with the observational dataset is ensured. Downscaled variables include 2-m maximum and minimum temperature, 2-m maximum and minimum relative humidity, 10-m zonal wind, downward short-wave radiation, 2-m specific humidity, and precipitation accumulation all at a daily time step. There are two versions of MACA data; the difference between them pertains to epoch adjustments for variables and periods, while removing the trend. For this study, MACA version 2 was used.

The two sources provide outputs from different GCMs under different RCP scenarios. GDO provides values for RCPs 2.6, 4.5, 6, and 8.5 from 40 GCMs, whereas MACA has output for RCP 4.5 and 8.5 from 20 GCMs. For this study, nine GCMs common to both climate databases were selected for preliminary assessment (Table 1) to allow for comparison. Analysis, comparisons, and evaluations were performed using climate projections from 1966 to 2005 for GDO and MACA and observed ground-based weather station data. A prior analysis published in [27] indicated an increasing trend in precipitation depth from 1966 forward, so we selected 1966 as the beginning year in our analyses.

Table 1. Different GCM models used for quantifying the error or bias when compared with the ground-based station from NOAA's (National Oceanic and Atmospheric Administration) Climate Data Online facility.

S. No.	GCM	Basic Source	Studies Based on Source
1	Beijing Climate Center Climate System Model, Beijing, China (BCCCSM)	http://forecast.bcccsm.ncc-cma.net/htm/	[33–36]
2	Community Climate System Model, USA (CCSM4)	http://www.cesm.ucar.edu/	[37–40]
3,4	Geophysical Fluid Dynamic Laboratory, USA (GFDL_ESM2G and GFDL_ESM2M)	http://nomads.gfdl.noaa.gov:8080/DataPortal/cmip5.jsp	[1–3,41–43]
5,6	Institute Pierre Simon Laplace Climate Modeling Center, France (IPSL_CM5ALR and IPSL_CM5AMR)	http://icmc.ipsl.fr/	[4,5,44,45]
7,8	MIROCESM and MIROCESMCHEM, Japan	http://www.geosci-model-dev.net/4/845/2011/	[6,7,46,47]
9	Norwegian Earth System Model, Norway (NorESM1M)	http://adsabs.harvard.edu/abs/2013GMD.....6..687B	[8,9,48,49]

2.3. Data Analysis

Data for the historical period obtained from the two sources were compared with observed data from the three ground-based climate stations for 1966–2005 obtained and quality checked under NCDC: NOAA protocol (https://www.ncdc.noaa.gov/cdo-web/datasets and https://www1.ncdc.noaa.gov/pub/data/cdo/documentation/GHCND_documentation.pdf). Data analysis included comparisons of means and distributions of the observed data and simulated values. Beyond the statistical properties, we computed conditional probabilities for precipitation, and various extreme and general climate indices (Table 2). For both sources, each model was considered individually (as opposed to using ensembles) so as to capture the range of possible values consistent with [50]. Comparisons were performed to quantify the error in simulated values in terms of their distributions, statistical properties, and climate indices including extremes. Other measures of performance included skill scores and Cohen's Effect Size (Cohen's d) as described in Table 2. All measures were used to evaluate the performance of each data source and the different methods of bias correction. For this study, a day with precipitation less than 0.1 mm was considered a dry day and any day with precipitation depth $\geq$0.1 mm was considered a wet day based on our previous study [27] and other literature review [10–15,51–56].

The analysis began by comparing GDO and MACA values with the observed data for the three ground-based stations from the National Climatic Data Center (NCDC). The source that performed better in simulating climate values was selected and then treated with different bias correction methods that were chosen after extensive review of literature [15,57,58]. Care was taken to preserve the means and variances. One method was a conventional one that included power transformation [57,58] and variance scaling of temperature [59]. The other bias correction method was novel and based on conclusions and discussions from previous studies [27,60] where Stochastic Weather Generators (SWGs) performed better at simulating greater depths of precipitation. We postulated that SWGs could be used to redistribute the precipitation and simulate greater daily precipitation depths. This precipitation might otherwise be distributed to dry days or days with lower or no precipitation, thus, adversely affecting simulation outputs from crop growth and hydrologic models.

To evaluate the performance of SWGs for bias correction, climate values from the better performing climate projection source were used as input to two SWGs—CLimate GENerator (CLIGEN) [61] and the Long Ashton Research Station Weather Generator (LARS-WG) [62,63]—both of which have been evaluated and found suitable for use in hydrologic and water resources studies in previous work by the authors [27]. The weather generators were used in their default state without changing their parametrization. Twenty-five different realizations [60] were generated for all nine GCMs at the three stations, to capture the variability and correct for bias or reduce error. Since the interest was to redistribute the precipitation to capture high magnitude precipitation events, the 75th and 90th percentiles precipitation values from the 25 different realizations were used for precipitation depth comparisons and means were used for temperature comparisons. This was because precipitation is not normally distributed, but temperatures are. The 75th percentile or interquartile range (as 50th percentile was zero) and 90th percentile were expected to pick up extreme precipitation events (which were not captured by GCMs). The 75th and 90th percentile values were selected because variations between simulated and observed precipitation were found to start after the interquartile range and increase at the 90th percentile and beyond, with the largest variations being observed at higher percentiles [27].

Following the evaluation of the different bias correction methods, the best approach was used to develop correction factors using the historic period and was translated to the climate projections from the different climate models for the eight stations in Figure 1. The reliable climate projections so generated can be used to evaluate changing climate impacts on water resources in the WLEB. Methodology in this study can be extended to any study site. The summary of the methodology is explained via flowchart in Figure 2B.

Table 2. List with explanation, application, and computational formula for various climate indices, verification skill scores, and performance coefficients.

CLIMATE INDICES		
Parameter Name	**Definition**	**Application**
Count of Dry Spell [10–14,51–55]	A period with at least 15 consecutive days in which none of the days had greater than 0.1 mm of rainfall	Onset and cessation of droughts can be projected using count of dry spells. Moreover, dry spell affect aquatic biodiversity, crop growth, and hydropower generation.
Count of Wet Spell [15,56]	A period where there were more than three wet days (day with precipitation more than or equal to 0.1 mm) ended with two continuous dry days (day with precipitation less than 0.1 mm)	Information on wet spell is important for optimizing water allocation and distribution, which is instrumental in planning flood control remedies and regulating sediment yield into the main streams.
Number of dry and wet day count in a month	Absolute count of days with precipitation depth of less and more than 0.1 mm on a single day	The decision on beginning planting of a crop based on crop water requirements is dependent on count of number of dry and wet days in a month.
Number of Snow Days [16,17,64,65]	Day with average temperature lower than 2 °C and precipitation depth more than 0.1 mm	The water budget of snow dominated watershed is dependent on count of snow days.
Growing Season Requirement/ Period of optimal growth [18–20,66]	Day with an average temperature between 20 and 25 °C (supports corn growth in Midwest USA)	Estimation of growth and yield of corn requires information on period of optimal growth of corn
Growing Degree Days (GDD) or Heating Units (HU) [18,66]	Heating Units (HU) are energy (heat) units affecting crop cycle from planting till harvesting.	$\mathrm{GDD} = \frac{\text{Maximum Temperature} + \text{Minimum Temeprature}}{2} - \text{Base Temperature}$ Different stages of crop growth cycle can be simulated using information on Heating Units (HU).
Count for Maximum Dry and Wet Length [21,67]	The longest continuous stretch of the dry and wet period	Information on this data helps in identifying extreme events, including dry and wet periods
Probability of dry day (Pd)	All these factors are critical in generating long-term climate simulation, hence needed evaluation. Moreover, mean length of dry and wet period decides onset of planting and harvesting in rainfed agricultural places. (for the transition probabilities computation, the dry day is day with the precipitation 0.1 mm and anything equal and more than 0.1 mm is wet day for all other purposes, the threshold 0.1 mm)	$\mathrm{p_d} = \frac{\text{Number of dry days}}{\text{Total number of days}}$
Probability of wet day (Pw)		$\mathrm{p_w} = \frac{\text{Number of wet days}}{\text{Total number of days}} = 1 - \mathrm{p_d}$
Probability of dry followed by dry day (Pd ǀ d)		$\mathrm{p_{d\|d}} = \frac{\text{Number of sequence with two dry days}}{\text{Total number of dry days}}$
Probability of wet day followed by wet day (Pw ǀ w)		$\mathrm{p_{w\|w}} = \frac{\text{Number of sequence with two wet days}}{\text{Total number of wet days}}$
Probability of wet day followed by dry day (Pw ǀ d)		$\mathrm{p_{w\|d}} = 1 - \mathrm{p_{d\|d}}$
Probability of dry day followed by wet day (Pd ǀ w)		$\mathrm{p_{d\|w}} = 1 - \mathrm{p_{w\|w}}$
Average length of dry and wet period (Ld, and Lw)		$\mathrm{L_d} = \frac{1}{\mathrm{p_{w\|d}}} \mathrm{L_w} = \frac{1}{1-\mathrm{p_{w\|w}}}$
Return time Period to have an event equal to average length of dry and wet period (Td and Tw) [22,23,68,69]		$\mathrm{T_d} = \frac{1-\mathrm{p_{w\|w}}+\mathrm{p_{w\|d}}}{\text{Number of days in a month} * \mathrm{p_{w\|d}}\left(1-\mathrm{p_{w\|w}}\right)\left(1-\mathrm{p_{w\|d}}\right)^{\mathrm{L_d}}} \mathrm{T_w} = \frac{1-\mathrm{p_{w\|w}}+\mathrm{p_{w\|d}}}{\text{Number of days in a month} * \mathrm{p_{w\|d}}\left(1-\mathrm{p_{w\|w}}\right)\mathrm{p_{w\|w}}^{\mathrm{L_d}}}$
One day maximum Precipitation (mm) [24,25,70,71]	Maximum value of single day precipitation event	Drainage design, soil conservation and management, risk mitigation, in events, including flash floods and droughts

Table 2. *Cont.*

VERIFICATION PARAMETERS			
Parameter Name	**Definition**	**Formula**	**Range**
Lorenz Curve [26,72]	Daily precipitation totaled data are arranged in increasing order, cumulative, and converted to a proportion of total precipitation		
Brier Score [27,73]	Measures the mean squared probability error	$$BS = \frac{1}{n}\sum_{i=1}^{n}(f_i - o_i)^2$$ Where f_i are forecast probabilities between 0 and 1 and oi are given as 0 and 1 for observed dry and wet days, respectively.	Lower brier score means the forecast is closer to the observation. BS can be partitioned into three terms: (1) reliability, (2) resolution, and (3) uncertainty.
Bias [28,74]	Verification metric denoted by ratio of total number of events forecast and total number of events observed; Forecast is termed as underforecast when BIAS < 1 or overforecast (BIAS > 1) events	$$\text{Bias} = \frac{h+f}{h+m}$$ Where h = Hit, f = False Alarm, m = miss	Perfect Score: 1
Extreme Dependent Score [29,75]	EDS is independent of bias, so should be presented together with the frequency bias	$$EDS = \frac{\ln p - \ln H}{\ln p + \ln H}$$ Where p = (hits + misses)/total is the base rate (climatology), H is the hit rate, also known as the probability of detection, and F is the false alarm rate, also known as the probability of false detection.	[−1, 1], 0 indicating no skill with 1 representing perfect score.
Cohen's-d effective size [30–32,76–78]	Alternate measure of checking the differences in distributions	$$\text{Cohen's d} = \frac{M1 - M2}{SD_{cont}}$$ Where M1 and M2 are means from the simulated and observed data and SD control is standard deviation from observed data or pooled standard deviation generally used with more realizations.	Values closer to 0 correspond to better simulations. In general, d = 0.2 (small); d = 0.5 (medium); and, d = 0.8 (large) effect sizes

3. Results

3.1. Comparison of Data from Two Different Sources of Climate Projections (GDO and MACA)

Density distribution plots for monthly precipitation for the period from 1966 to 2005 (Figure 3a, Figure S1A,B) showed that performance of datasets from both climate projection sources was similar. The GCMs tended to distribute precipitation across more periods than what was evident from observed data. For example, some models simulated more months having precipitation totals between 20 mm and 100 mm than what was seen for the observed data (highlighted in the red box in Figure 3a). Some models overestimated months having precipitation totals of more than 100 mm (both models). MACA had a wider range of simulation outputs from the different GCMs compared to GDO. At Adrian, MI, MACA-based simulations did not perform well in capturing lower values of annual precipitation totals during the late 1970s and 1980s, whereas GDO-based projections did not capture higher values of annual precipitation totals around the mid-1970s and late 1990s (red boxes in Figure 3b). Similar patterns were seen at the other two stations (Figure S1A,B).

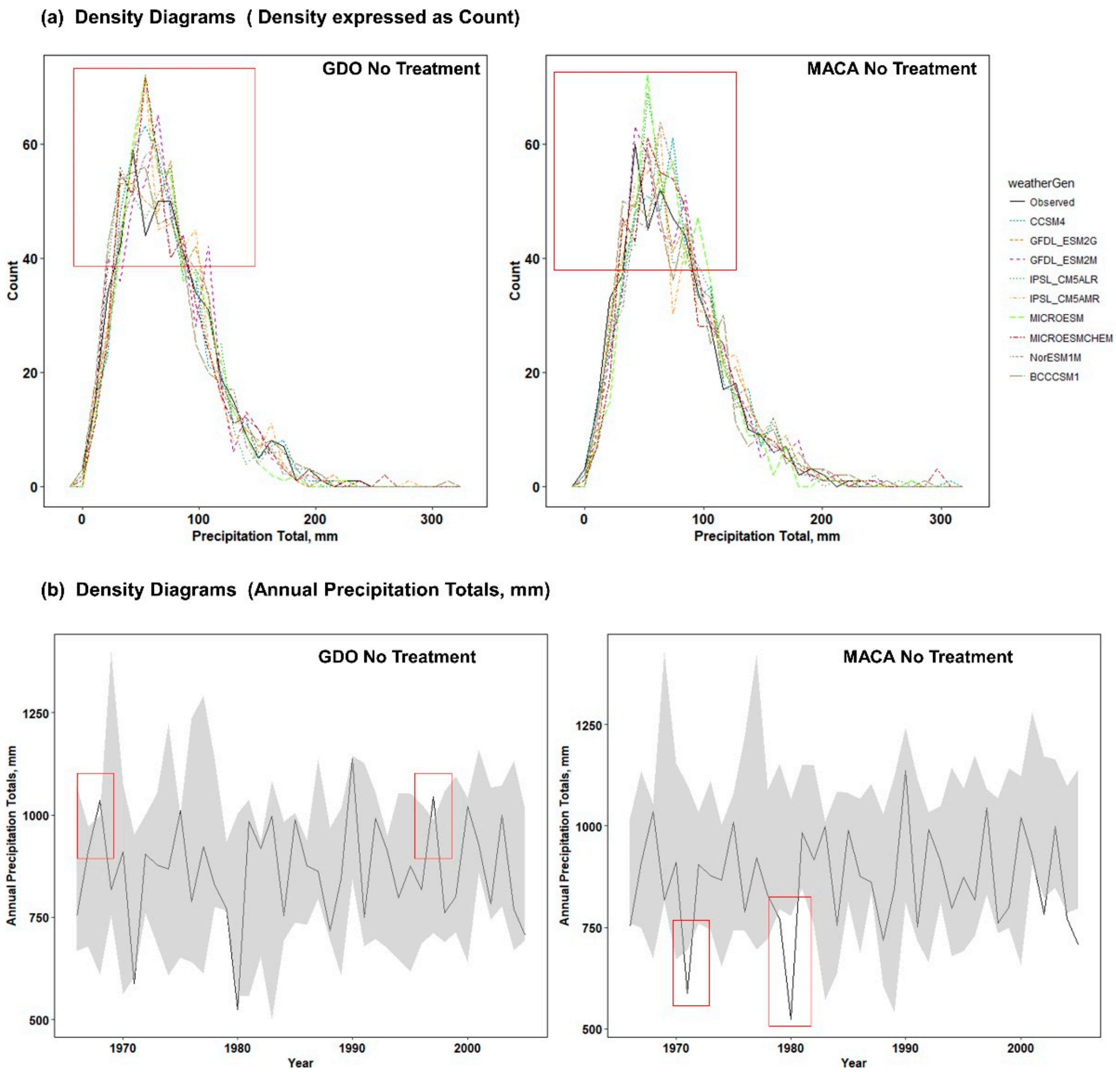

Figure 3. (**a**) Density distribution charts for Adrian, MI for monthly precipitation depths, mm; (**b**) Annual precipitation depths, mm, with range bounds from different GCM outputs. (Charts for Fort Wayne, IN and Norwalk, OH are presented in Figure S1A,B.)

Comparison of statistical properties from all different GCMs from the two different climate projection sources (Table 3 and Table S1) showed that both sources performed equally well in simulating mean and minimum values of daily precipitation depth at all three stations. Neither source was able to capture the number of days with zero precipitation depth (NDPO) although MACA performed better than GDO, and similarly for maximum precipitation values. However, GDO values of maximum precipitation were closer to observed values at Adrian, MI, with values ranging from 65.4 mm to 110.1 mm compared with 120.4 mm from the observed data. Overall, MACA-based simulations were better at capturing the statistical properties of precipitation data.

Analysis of wet days (Table S2) showed a tendency to overestimate the number of wet days in a month (both sources), although MACA-based simulations performed better. This would explain why one-day maximum precipitation values from both sources failed to match observed values as rainfall was spread across more days hence overall lower values were simulated. Values from MACA-based simulations were close to observed values in some of the months (e.g., 11 days in February at Fort Wayne, IN compared with 10 days from observed data and 17 days from GDO output). MACA-based values were particularly better at Fort Wayne, IN, where the observed value was captured in one of the months (November) and simulated values were within two days of observed values in seven of the months. The number of wet days in a month based on the GDO source were generally greater (5–15 days more than observed) than what was obtained based on the MACA source (0–7 days more than observed) for all three stations. Results obtained for the number of dry days in a month (Table S3) were similar to those for wet days in a month for both sources. Generally, both sources underestimated the number of dry days in a month although MACA performed better. This was not surprising as both sources had overestimated the number of wet days in the month. MACA-based values came very close to observed values (within 1–2 days) in seven of the months and matched observed values in November at Fort Wayne, IN, similar to observations for number of wet days in a month. Values from GDO-based simulations performed particularly poorly in April through August at Fort Wayne, IN and over most months at Norwalk, OH.

The analysis of extreme and general climate indices (Figure 4, Table S4 and Table 4) showed that MACA-based data captured maximum dry length very well while this value was underestimated by GDO for all three stations. The number of dry sequences were also severely underestimated for both sources. Values for maximum wet lengths were overestimated for both sources (larger values were seen with GDO outputs) with the exception of MACA at Norwalk, OH for which the observed value was well captured within the range of values obtained. The number of wet sequences was, however, greatly overestimated for both sources (377–501 compared with 153–183 for the observed data). This corresponds to previous observations regarding the tendency of the models to spread precipitation across a larger number of days than what would generally occur based on observed data. Transitional probabilities were generally captured well by MACA outputs but values from GDO outputs at all three stations indicated that this climate dataset lacked much needed accuracy. The mean lengths of the dry periods were well captured in MACA-based data at Fort Wayne, IN and Norwalk, OH, but underestimated otherwise. Neither source was able to capture the mean length of the wet period (Lw) although values were closer for MACA. Return periods for the mean lengths of dry periods were overestimated by both GDO and MACA sources, with GDO values being substantial larger than observed (Table 4). Return periods for the mean lengths of wet periods were underestimated by both sources although differences were not very large. Overall, MACA-based values were better at capturing both extreme and general climate indices.

Table 3. Comparison of GDO and MACA climate projection sources for Adrian, MI, Fort Wayne, IN, and Norwalk, OH in simulating descriptive statistics for daily precipitation (mm), and maximum and minimum air temperatures (°C).

	Adrian, MI			Fort Wayne, IN			Norwalk, OH		
	Precipitation, mm								
Treatment	**Median**	**NDP0 * (%)**	**Maximum**	**Median**	**NDP0 (%)**	**Maximum**	**Median**	**NDP0 (%)**	**Maximum**
Observed	0	66.9	120.4	0	63.5	111.8	0	64	229.1
GDO	(0.2–0.2), 0.2	(29.8–31.9), 30.9	(65.4–110.1), 83.3	(0.4–0.5), 0.4	(15.4–20.7), 17.7	(52.0–72.0), 63.7	(0.7–0.8), 0.8	(10.8–13.0), 12.0	(40.1–48.0), 43.6
MACA	(0.0–0.0), 0.0	(53.5–54.1), 53.9	(67.2–71.0), 69.7	(0.0–0.0), 0.0	(54.6–55.5), 54.9	(65.0–74.5), 72.3	(0.0–0.0), 0.0	(51.0–51.7), 51.4	(54.5–112.8), 101.6
	Maximum Temperature, °C								
Treatment	**NDT35 † (%)**	**Maximum**	**Minimum**	**NDT35 (%)**	**Maximum**	**Minimum**	**NDT35 (%)**	**Maximum**	**Minimum**
Observed	0.3	40.0	−20.0	0.3	41.1	−23.9	0.2	39.4	−22.2
GDO	(0–0.4), 0.2	(36.0–38.9), 37.4	(−20.4–−16.2), −18.5	(0.1–0.5), 0.3	(36.7–39.5), 38.1	(−23.2–−17.4), −19.7	(0–0.3), 0.1	(34.8–39.8), 36.9	(−21.3–−14.9), −18.2
MACA	(0.5–0.7), 0.6	(39.5–40.2), 39.9	(−17.5–−16.5), −17.1	(0.5–0.8), 0.7	(40.6–42.1), 41.8	(−22.1–−20.3), −21.4	(0.2–0.3), 0.2	(37.6–37.8), 37.7	(−19.2–−17.8), −18.8
	Minimum Temperature, °C								
Treatment	**NDT2 ‡ (%)**	**Maximum**	**Minimum**	**NDT2 (%)**	**Maximum**	**Minimum**	**NDT2 (%)**	**Maximum**	**Minimum**
Observed	46.3	24.4	−30.0	41.1	25.6	−30.0	41.8	25.0	−29.4
GDO	(44.4–46.0), 45.4	(21.7–26.3), 23.6	(−31.2–−25.8), −29.0	(39.5–41.2), 40.3	(22.7–26.8), 25.0	(−33.8–−26.8), −30.2	(39.9–41.6), 40.9	(22.0–27.8), 24.6	(−29.7–−23.6), −27.2
MACA	(44.8–45.7), 45.3	(23.8–24.0), 24.0	(−28.2–−26.4), −27.9	(39.9–40.7), 40.4	(25.2–25.5), 25.5	(−28.9–−26.9), −28.4	(41–41.6), 41.4	(24.0–24.0), 24.0	(−28–−27), −27.5

* NDP0: Number of days with daily precipitation depth 0 mm expressed as percentage of total days of observation. † NDT35: Number of days with daily maximum air temperature 35 °C expressed as percentage of total days of observation. ‡ NDT2: Number of days with daily maximum air temperature 2 °C expressed as percentage of total days of observation. Values in the table are presented as (Minimum of values from all 9 GCMs—Maximum values from all 9 GCMs), Median of values from all nine GCMs.

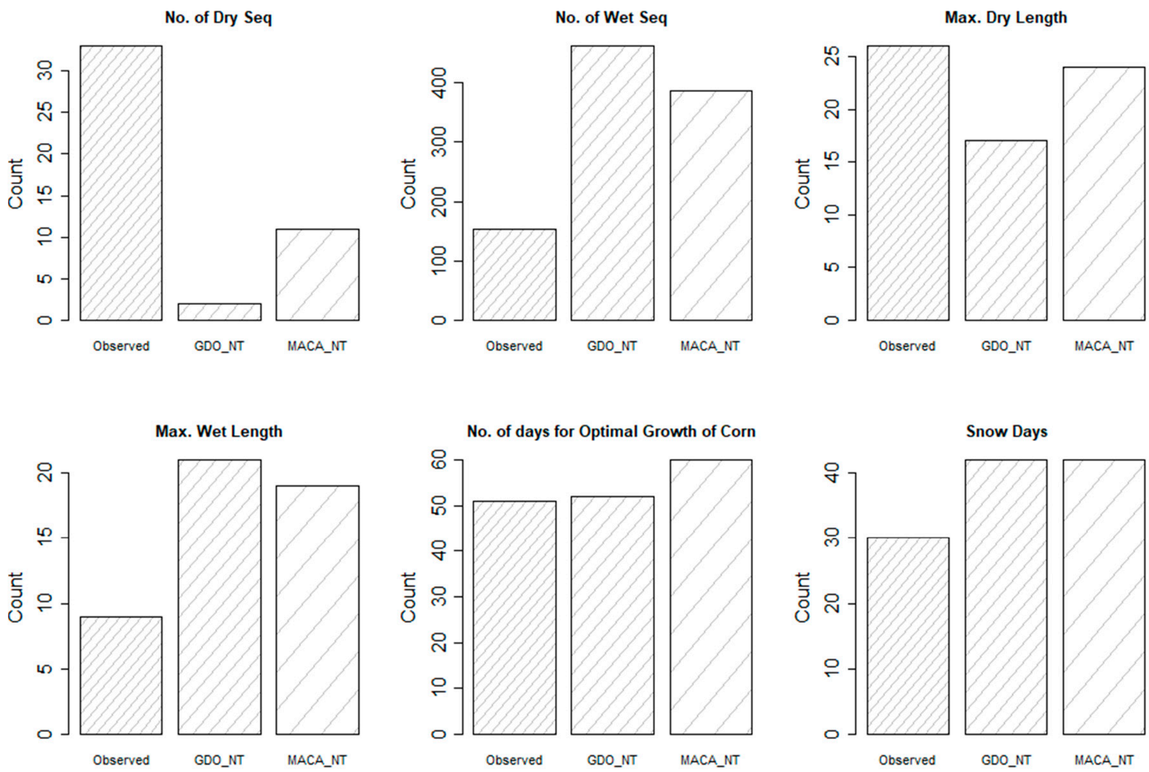

Figure 4. Comparison of GDO and MACA climate projection sources while simulating different climate indices for Adrian, MI between 1966 and 2005 (GDO_NT: GDO No Treatment; MACA_NT: MACA No Treatment). Plots for Fort Wayne, IN and Norwalk, OH can be seen in Figure S3A,B.

Table 4. Comparison of GDO and MACA climate projection sources for different climate indices for Adrian, MI, Fort Wayne, IN, and Norwalk, OH for 1966 to 2005.

	Index					
Treatment	**P(w∣w)**	**P(w∣d)**	**Ld**	**Lw**	**Td**	**Tw**
	Adrian, MI					
Observed	0.5	0.3	4	1	1	4
GDO	(0.7–0.7), 0.7	(0.5–0.6), 0.5	(2–2), 2	(2–2), 2	(13–33), 21	(1–1), 1
MACA	(0.6–0.6), 0.6	(0.3–0.4), 0.3	(3–3), 3	(2–2), 2	(2–3), 2	(1–2), 1
	Fort Wayne, IN					
Observed	0.5	0.3	3	1	1	3
GDO	(0.8–0.8), 0.8	(0.6–0.7), 0.6	(2–2), 2	(3–3), 3	(52–174), 81	(1–1), 1
MACA	(0.6–0.6), 0.6	(0.3–0.3), 0.3	(3–3), 3	(1–2), 2	(2–2), 2	(1–2), 1
	Norwalk, OH					
Observed	0.5	0.3	3	1	1	3
GDO	(0.9–0.9), 0.9	(0.7–0.8), 0.7	(1–2), 1	(3–4), 4	(256–2016), 738	(1–1), 1
MACA	(0.6–0.6), 0.6	(0.3–0.4), 0.4	(3–3), 3	(2–2), 2	(2–3), 3	(1–1), 1

Daily air temperature analysis (Table 3, Tables S5 and S6) revealed that both sources performed well and at par with respect to the statistical properties for maximum and minimum air temperature for all three stations. This is consistent with [50], based on which the expectation is that biases with respect to temperatures would be minimal regardless of the source of projections. That said, the number of days with maximum temperature greater than 35 °C and, in general, values related to minimum temperatures were better represented by GDO data. The number of days for optimum growth of corn was better represented by GDO at Adrian, MI (Figure 4) and by MACA at Fort Wayne, IN and Norwalk, OH (Table S4). For example, at Fort Wayne, IN, the GDO source output estimated 67–76 days for optimum corn growth, while the MACA source output estimated 63–67 days; compared with 63 days from observed data (Table S4). Output from both sources overestimated the number of snow days with the closest representation being from MACA output at Fort Wayne, IN for which the range of values was 34–37 days compared with 33 days based on observed data. Values from GDO tended to be greatly overestimated, for example 63–71 days at Norwalk, OH, compared with 31 days from observed data (Table S4). The number of growing degree days (Table S7) were generally well captured by outputs from both sources with the exception of values for 15 October, which were often overestimated by over 100. Values based on GDO were also overestimated for 1 October at Fort Wayne, IN and Norwalk, OH.

Forecast verification or skill scores along with performance coefficients for precipitation events showed that GDO had a higher Brier score (0.6) than MACA (0.5) for Norwalk, OH; this indicated that GDO projections were relatively more offset from the observed data than MACA. Higher bias was recorded for GDO (1.7, 1.8, and 2.1 at Adrian, Fort Wayne, and Norwalk, respectively), when compared with 1.4, 1.2, and 1.3 for the MACA source at the three stations, respectively. Lower EDS score for MACA (0.2, 0.1, and 0.2 Adrian, Fort Wayne, and Norwalk, respectively compared with 0.3, 0.4, and 0.6, respectively for GDO) showed that there was greater dependence between the projected GDO output and observed data and the GDO forecast was less random. No high correlations were seen between projected values from either source and the observed data. Relative performance of both climate projection sources was the same for growth degree days at all stations. From the outputs discussed, the MACA source performed better than GDO in most of the parameters. Therefore, the MACA source was selected for further analysis to correct biases. Corrections were not necessary for temperatures since these were well captured by default outputs.

3.2. Evaluation of Different Bias Correction Methods for the Historic Period

Climate values from different outputs from the MACA source were treated with different methods of bias correction, including conventional methods (power scaling for precipitation and variance scaling of temperature) and SWGs. The Q-Q plots between simulated values and observed data (Figures 5–7) revealed that power transformation redistributed the precipitation fairly well and provided better representation of daily precipitation albeit with a slight overestimation at the higher values. None of the SWG-based approaches performed well at any of the stations based on these figures. Statistical properties evaluated at a daily time step (Table S8) showed that power transformation greatly improved the representation of precipitation for MACA-based simulations. For example, values of standard deviation and daily maximum precipitation at Adrian ranged from 6.5–6.6 and 116.6–134.3 mm, respectively after power transformation, compared with 6.5 and 120.4 mm, respectively based on observed data, having improved from values obtained before transformation (5.4–5.7 and 67.2–71.0 mm, respectively). A similar picture was seen at the other two stations and for other properties such us skewness (both) and kurtosis (Norwalk, OH). Means, medians, and minimums were generally captured well at all stations, with or without power transformation. For SWG-based corrections, the LARS-WG 75th percentile was able to capture mean and minimum values relatively well, but otherwise failed on all other properties. None of the other SWG-based corrections were able to provide suitable representation of precipitation at any of the stations.

Evaluations on a seasonal basis (Table S8) showed that power transformation greatly improved the representation of precipitation for MACA-based simulations at all three stations. The improvements were especially evident in the spring and summer and with values of maximum precipitation within seasons. As with daily values, the LARS-WG 75th percentile was able to capture mean and minimum values relatively well at the seasonal level, but otherwise failed on all other properties. None of the other SWG-based corrections performed well at this level, with the exception of minimum values, which all but LARS-WG 90th percentile were generally able to capture. None of the treatments was able to capture the number of days with no precipitation, with the exception of power transformation at Norwalk, OH for the fall season, which came close (59–62% compared with 62.9% for the observed data).

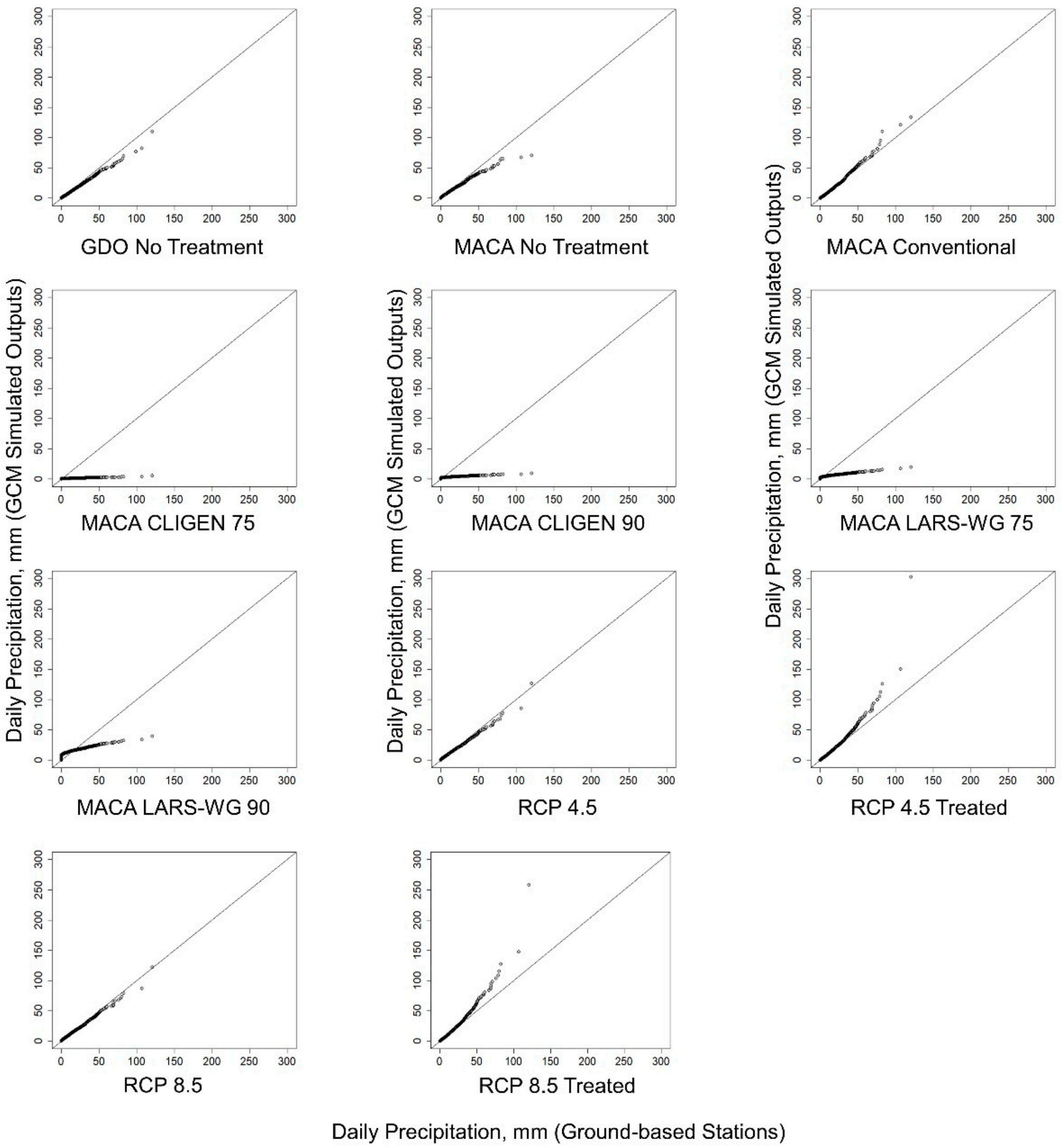

Figure 5. Q-Q plots to evaluate the performance of different bias correction methods for period between 1966 and 2005 to reduce the bias in simulating values for daily precipitation, mm and to present the future climatic scenarios (2006–2099) for Adrian, MI.

Analysis of extreme and general climate indices (Table 5) showed that the maximum length of dry periods was captured relatively well by MACA outputs at all stations with or without power transformation, as was the maximum length of a wet period at Norwalk, OH. For example, maximum dry period length at Adrian, MI ranged between 17–29 days without treatment and 17–32 days with treatment, compared with 26 days obtained from observed data. The representation of the maximum length of a wet period was generally the same for treated and untreated data. The average length of a dry period was better captured with power transformation at Fort Wayne, IN and Norwalk, OH and values at Adrian, MI improved with the transformation (2.8–3.2 days with transformation compared with 1.7–1.9 days without transformation and four days for the observed data). No changes were seen in the average length of the wet period, and in the return periods for either the dry or wet periods following transformation. The number of snow days was better represented by the original MACA dataset (no treatment) at all stations, although values were generally overestimated.

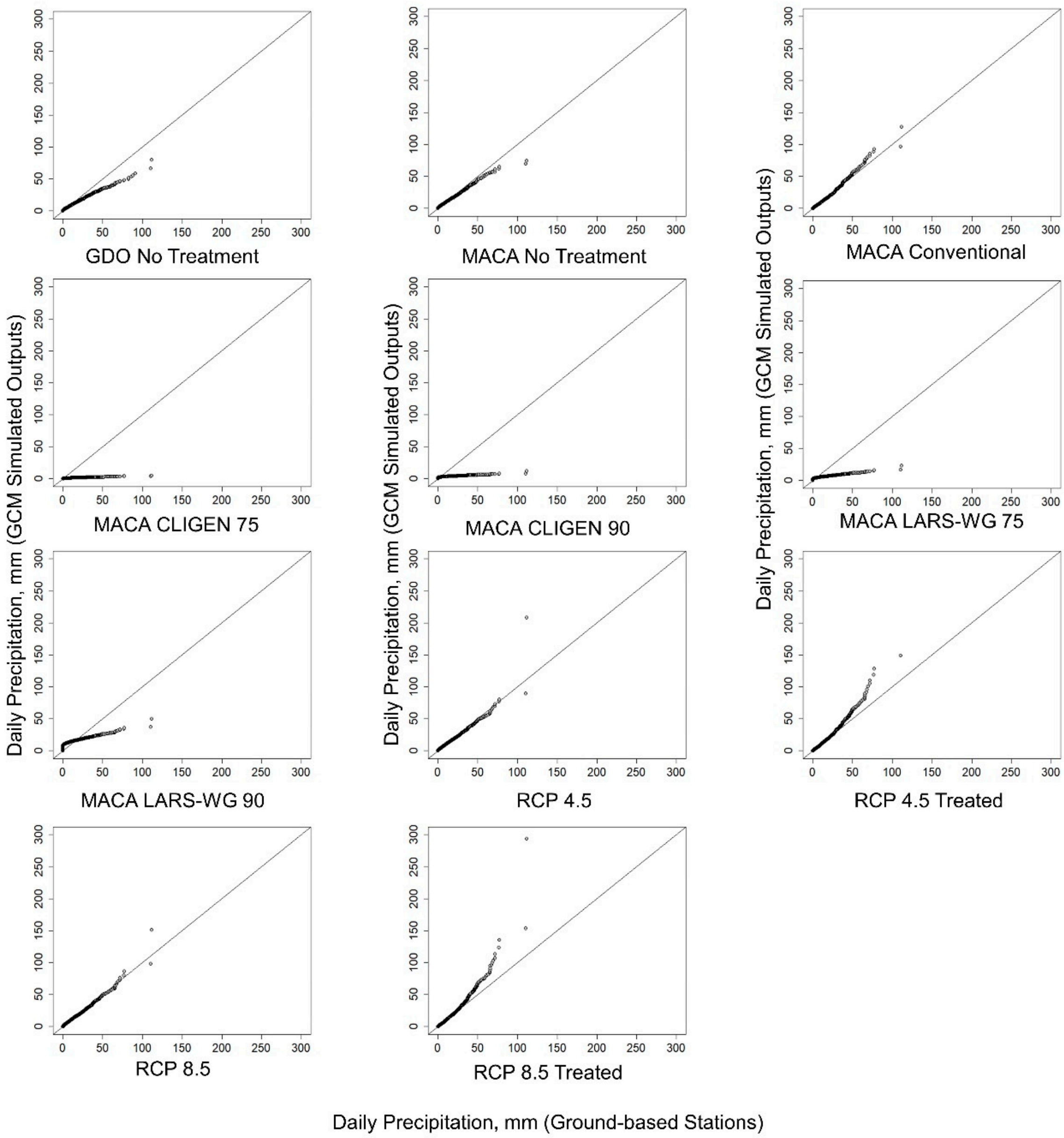

Figure 6. Q-Q plots to evaluate the performance of different bias correction methods for the period between 1966 and 2005 to reduce the bias in simulating values for daily precipitation, mm and present future climate scenarios (2006–2099) for Fort Wayne, IN.

Distributions obtained using Lorenz curves (Figure 8) showed that power transformation reduced the bias and projected similar distributions as those observed from the ground-based stations. Values of Cohen's effect size, d for power transformation ranged from 0.1–0.3 indicating that differences between treated data and observed values were small. Values obtained for SWGs were mixed indicating that the SWG simulation outputs were less close to the observed data, consistent with previous observations. The bias was also higher when using the SWGs (2.6–3.0) compared to power transformation (1.2–1.4).

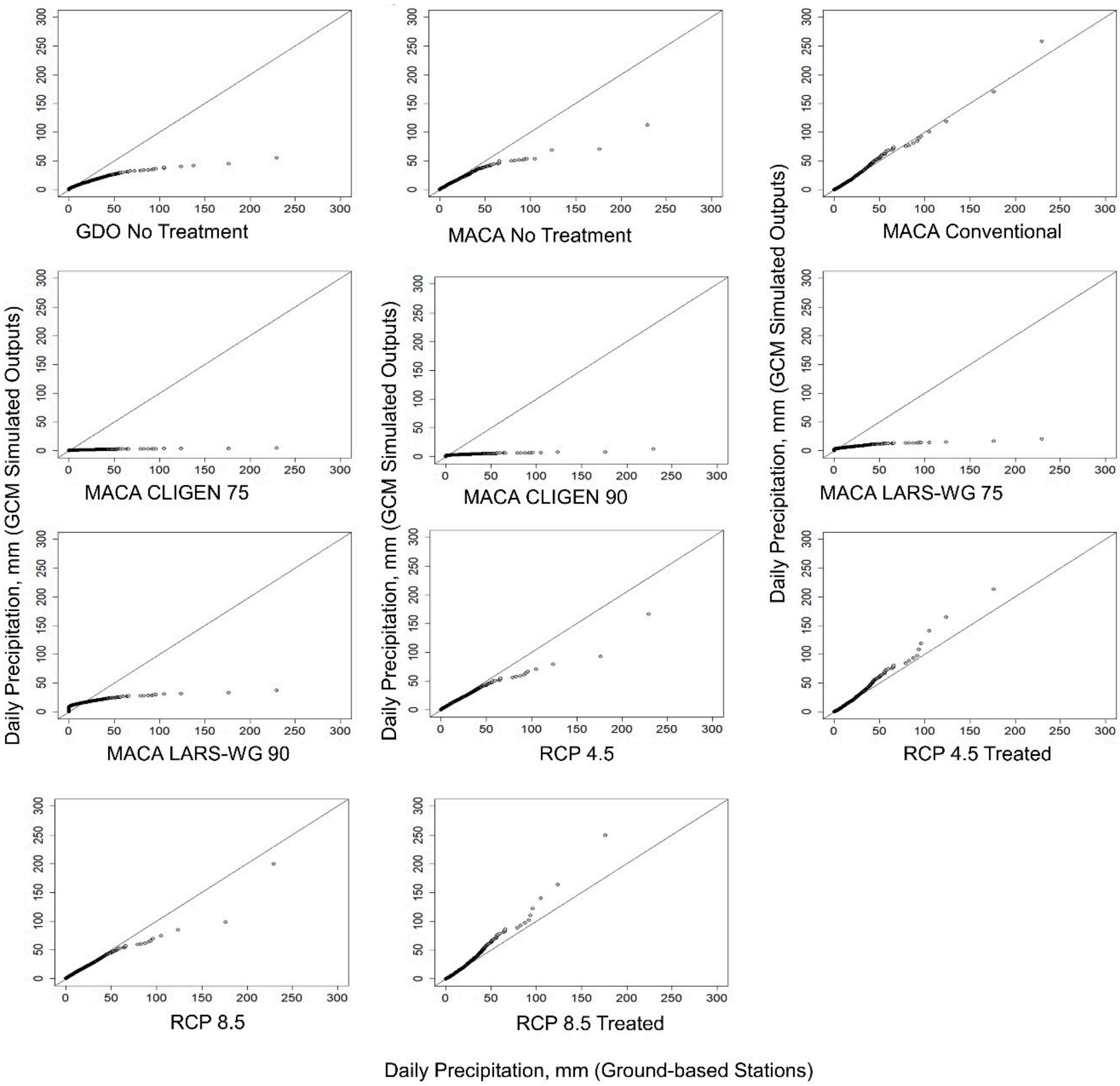

Figure 7. Q-Q plots to evaluate the performance of different bias correction methods for period between 1966 and 2005 to reduce the bias in simulating values for daily precipitation, mm and to present the future climatic scenarios (2006–2099) for Norwalk, OH.

Overall, results indicated that power transformation outperformed any other method of bias correction in this study. Generally, SWGs did not perform well as methods of bias correction, with the exception of LARS-WG 75th percentile, which captured mean values relatively well (Table S4) and CLIGEN 75, which captured the maximum and average lengths of dry periods and the number of wet sequences relatively well (Table 5). The potential of weather generators as tools for bias correction has previously been discussed [79] and such generators have been used to generate reliable future climate datasets [80]. Thus, the possibility of using SWGs for bias correction cannot be completely discarded.

As previously noted (Section 3.1), precipitation suffered from the most bias, while maximum and minimum temperature had minimal bias and did not require much, if any, correction. The Q-Q plots drawn from outputs of different climate models when treated with the different bias correction methods (Figure S2A–F) showed that the SWGs and variance scaling of temperature did not perform well in correcting any biases. Default values from either GDO or MACA had less bias and could be used without correction, consistent with previous conclusions.

Table 5. Extreme event and general climate indices analysis for Adrian, MI; Fort Wayne, IN; and Norwalk, OH for MACA climate projections before and after different bias correction methods compared with observed climate data from ground-based stations.

Treatment	Maximum Dry Length	Maximum Wet Length	Number of Dry Sequence	Number of Wet Sequence	Snow Days	Ld †	Lw †	Td †	Tw †
Adrian, MI									
Observed	26	9	33	153	30	4	1	1	4
MACA No Treatment	(17–29), 22	(16–23), 19	(4–17), 11	(318–450), 387	(40–43), 42	(1.7–1.9), 1.8	(1.5–1.6), 1.5	(1.9–2.5), 2.1	(1.3–1.5), 1.3
MACA Conventional	(17–32), 24	(15–23), 19	(4–19), 12	(314–446), 381	(60–62), 61	(2.8–3.2), 3	(1.5–1.6), 1.5	(1.9–2.5), 2.1	(1.3–1.5), 1.3
MACA CLIGEN75	(13–36), 23	(175–228), 210	(0–5), 2	(108–170), 142	(332–338), 335	(2.8–3.2), 3	(2.9–3.9), 3.2	(3084–2016), 767.2	(0.7–0.8), 0.7
Fort Wayne, IN									
Observed	30	11	16	166	33	3	1	1	3
MACA No Treatment	(22–37), 27	(15–29), 21	(8–23), 16	(310–432), 377	(34–37), 36	(1.5–1.7), 1.6	(1.4–1.5), 1.5	(1.7–2.3), 1.9	(1.3–1.5), 1.4
MACA Conventional	(22–37), 27	(14–29), 21	(309–432), 375	(309–432), 375	(42–44), 43	(2.9–3.3), 3.2	(1.4–1.5), 1.5	(1.7–2.3), 1.9	(1.3–1.5), 1.4
MACA CLIGEN75	(16–43), 26	(157–268), 213	(156–210), 194	(156–210), 194	(320–330), 324	(2.9–3.3), 3.1	(2.6–3.5), 2.9	(143–918.2), 301	(0.6–0.7), 0.6
Norwalk, OH									
Observed	25	18	15	183	31	3	1	1	3
MACA No Treatment	(16–29), 21	(14–27), 20	(2–15), 7	(346–473), 410	(38–41), 40	(1.3–1.5), 1.4	(1.5–1.6), 1.5	(2.2–3.1), 2.5	(1.1–1.3), 1.2
MACA Conventional	(18–29), 22	(13–27), 19	(322–456), 394	(322–456), 394	(50–53), 52	(2.6–3.0), 2.9	(1.5–1.6), 1.5	(2.2–3.1), 2.5	(1.1–1.3), 1.2
MACA CLIGEN75	(11–17), 15	(218–279), 243	(76–116), 100	(76–116), 100	(342–346), 345	(2.6–3.0), 2.9	(3.4–4.7), 4	(1260–8870), 3771.1	(0.9–1), 1

† Ld, Lw: average length of dry and wet period; Td, Tw: return period for average length of dry and wet period.

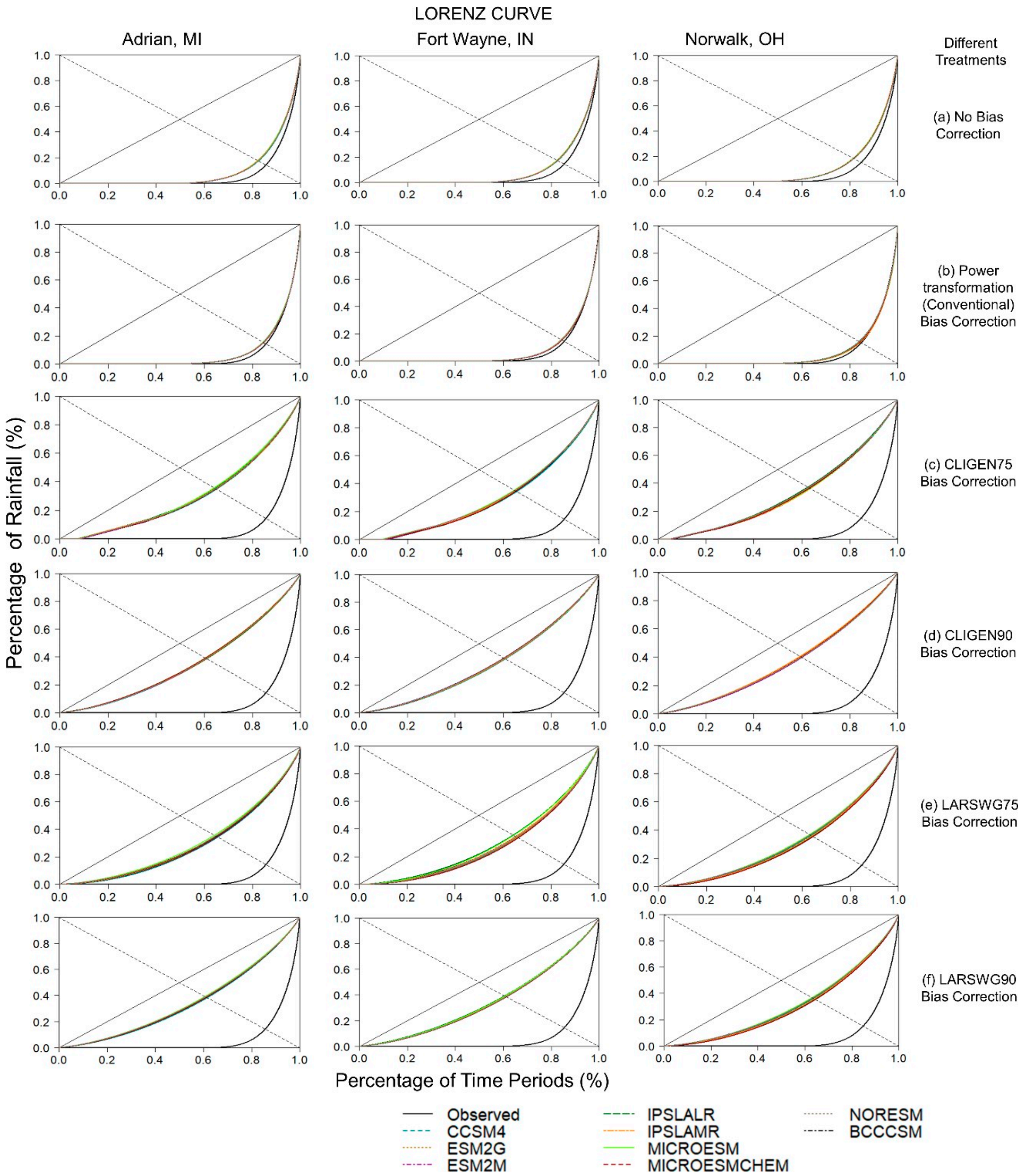

Figure 8. Performance evaluation of different bias correction methods for a historic period (1966–2005) in reducing the bias in the daily time series in simulating daily precipitation, mm for Adrian, MI; Fort Wayne, IN; and Norwalk, OH using Lorenz Curve.

3.3. Analysis of Climate Projections for Western Lake Erie Basin

Based on the analysis, only slight increases (0.1–0.4 mm) were expected in mean precipitation for either scenario. Not much difference was observed between the scenarios and values generally ranged from 2.4–2.9 mm compared with 2.4–2.6 mm obtained from observed data. No changes would be experienced in median values, which are expected to remain at 0 mm. The standard deviation was projected to increase by between 0.3 mm and 1.9 mm with highest increases expected at Norwalk, OH and the changes being about the same across both emission scenarios. Changes in scale parameters (in this case, the standard deviation) point to a rescaling of the distribution function [81] and, particularly in this case where the mean remains more or less constant, differences would be seen primarily at the tails, the shapes of which reflect the occurrence of extreme events. Extreme events are particularly sensitive to changes in scale with relative sensitivity being higher for larger extreme values, regardless of how the events respond to changes in location (in this case the mean) [81]. Based on our analysis, maximum precipitation is expected to increase at all stations and could be up to four times higher than that in the baseline scenario. For example, the maximum precipitation value at Fort Wayne, IN could go as high as 455 mm under RCP 4.5 compared with 111.8 mm from the baseline scenario. Higher increases are expected under the medium emission (RCP 4.5) scenario than under the high emission (RCP 8.5) scenario except at Norwalk, OH where maximum precipitation under RCP 8.5 could go as high as 540 mm based on projections (Table 6). Based on the analysis, increases in maximum precipitation will be especially evident during summer and spring (Table S9). The Q-Q plots of corrected daily precipitation for the future time series revealed that the magnitude of the maximum daily precipitation event would be much greater than that from the observed data (Figures 6–8), consistent with the previous observations. The maximum length of dry periods would remain the same or increase only slightly. The maximum wet length at Norwalk, OH would remain more or less the same under RCP 4.5 but could double or triple under RCP 8.5 (37–50 days compared with 18 days in the baseline scenario). Values of the maximum wet lengths at the other two stations and average lengths of both wet and dry periods at all three stations mirrored those from bias-corrected MACA-based simulations suggesting that no changes were expected in these values, and similarly for transitional probabilities.

Based on analysis of temperature projections (Table 7), mean maximum temperatures could increase by between 1.7 and 5.0 °C (average 2.6 and 3.8 °C under RCP 4.5 and RCP 8.5, respectively) across all stations in the basin, consistent with IPCC reports [82]. The largest changes in the absolute maximum value could be seen at Fort Wayne, IN, while increases in maximum temperature would be about the same at the other two stations, ranging between 1.6–12.8 °C (average 5.1–9.1 °C under RCP 4.5 and RCP 8.5, respectively). The number of days with temperatures >35 °C were projected to increase across the board, with the largest increases (1.7–10%) seen at Fort Wayne, IN. Increases at the other two stations were expected to be small although these could increase by up to 8.4% at Adrian, MI. Mean minimum temperatures could increase by between 1.8 °C and 5.0 °C (average 2.8 and 3.8 °C under RCP 4.5 and RCP 8.5, respectively) at all three stations. Absolute minimum temperatures could increase by up to 8.3 °C (average 3.4 and 5.0 °C under RCP 4.5 and RCP 8.5, respectively) although decreases of up to 1.5 °C could also occur. The number of days with temperatures <2 °C were projected to decrease across the board, with the largest decreases (5–18%) seen at Adrian, MI. This points to a potential decrease in the number of snow days as 2 °C is the threshold below which precipitation is more likely to fall as snow than as rain [16,64]. The growing degree days as projected will be sufficient for seeding, flowering and harvesting of corn. However, projected increases in GDD suggest that the growth period may shift 15 days earlier (Table 8). For example, the GDD on 1 May at Adrian, MI was projected to range between 98–142 under RCP 4.5 and 111–187 under RCP 4.5 compared with 60 and 104 on 1 May and 15 May, respectively obtained from the observed baseline data. Similar patterns were observed at the other two stations. Overall, GDD values were projected to increase at all three stations suggesting an overall longer growing period.

Table 6. Comparison of future climate scenarios (2006–2099) with the historical period (1966–2005) for daily precipitation, mm.

Treatment	Mean	Median	Std. Dev.	Maximum	Maximum Dry Length	Maximum Wet Length	Ld †	Lw †
Adrian, MI								
Observed	2.4	0.0	6.5	120.4	26	9	4	1
RCP4.5 Treated	(2.5–2.7), 2.6	(0–0), 0	(6.8–7.6), 7.3	(164.2–302.6), 214.4	(21–45), 27	(16–29), 20	(2.8–3.2), 3	(1.5–1.6), 1.5
RCP8.5 Treated	(2.5–2.8), 2.7	(0–0), 0	(6.8–7.9), 7.4	(157.5–258), 191.1	(20–46), 28	(17–26), 20	(2.8–3.4), 3.1	(1.4–1.5), 1.5
Fort Wayne, IN								
Observed	2.5	0.0	6.7	111.8	30	11	3	1
RCP4.5 Treated	(2.7–2.9), 2.7	(0–0), 0	(7.4–8.1), 7.7	(134.9–454.6), 213.2	(22–45), 30	(16–22), 18	(3.0–3.4), 3.2	(1.4–1.5), 1.5
RCP8.5 Treated	(2.6–2.9), 2.8	(0–0), 0	(7.3–8.3), 7.9	(151.5–293.8), 205.6	(27–41), 32	(15–26), 22	(3.0–3.5), 3.3	(1.4–1.5), 1.4
Norwalk, OH								
Observed	2.6	0.0	7.0	229.1	25	18	3	1
RCP4.5 Treated	(2.6–2.8), 2.7	(0–0), 0	(7.0–8.5), 7.7	(215.3–461.7), 324	(19–41), 27	(16–25), 20	(2.7–3), 2.9	(1.5–1.6), 1.5
RCP8.5 Treated	(2.6–2.9), 2.8	(0–0), 0	(7.1–8.8), 8.1	(255.4–536.9), 381.9	(22–34), 29	(37–50), 44	(2.7–3.2), 2.9	(1.5–1.6), 1.5

† Ld, Lw: average length of dry and wet period.

Table 7. Comparison of future climate scenarios (2006–2099) with the historical period (1966–2005) for maximum and minimum temperatures, °C.

	Maximum Temperature				Minimum Temperature			
Treatment	**Mean**	**Std. Dev.**	**Maximum**	**Days with Max > 35 °C (%)**	**Mean**	**Std. Dev.**	**Minimum**	**Days with Min < 2 °C (%)**
Adrian, MI								
Observed	15.0	11.5	40.0	0.3	3.1	10.0	−30.0	46.3
RCP4.5	(16.7–18.5), 17.7	(10.8–11.9), 11.5	(42.7–51.2), 45.8	(1.8–4.8), 3.1	(4.9–6.9), 5.8	(9.0–9.8), 9.4	(−31.5–−21.7), −26.8	(32.3–40.9), 38.1
RCP8.5	(17.6–20.0), 18.8	(11.2–12.1), 11.7	(46.2–52.6), 50.0	(3.6–8.7), 6.7	(5.7–8.1), 6.9	(9.2–10.2), 9.6	(−27.5–−22.6), −25.6	(28.4–39.2), 34.9
Fort Wayne, IN								
Observed	15.4	11.8	41.1	0.3	4.8	10.3	−30.0	41.1
RCP4.5	(17.0–19.0), 18.0	(11.1–12.1), 11.6	(45.2–53.9), 48.0	(2.0–5.1), 3.3	(6.3–8.4), 7.2	(9.5–10.1), 9.9	(−30.3–−23.3), −27	(28.5–36.4), 33.7
RCP8.5	(17.9–20.4), 19.2	(11.6–12.1), 11.9	(50.0–56.5), 52.4	(4.0–10.3), 7.3	(7.1–9.4), 8.3	(9.8–10.5), 10.1	(−28.6–−22.8), −26.3	(25.3–34.9), 31.1
Norwalk, OH								
Observed	15.0	11.4	39.4	0.2	4.4	10.1	−29.4	41.8
RCP4.5	(16.6–18.2), 17.5	(10.6–11.5), 11.1	(41.0–47.9), 43.9	(0.9–3.1), 2	(5.9–7.8), 6.8	(9.0–9.8), 9.4	(−30.9–−21.1), −26.6	(29.1–37.0), 34.5
RCP8.5	(17.5–19.5), 18.6	(10.8–11.6), 11.4	(44.8–52.2), 47.5	(2.5–6.4), 4.9	(6.8–9.0), 7.8	(9.2–10.1), 9.6	(−28.2–−21.9), −25.4	(25.1–35.6), 31.6

Table 8. Comparison of Growing Degree Days (GDD) under future climate scenarios (2006–2099) with those from the historical period (1966–2005) at Adrian, MI, Fort Wayne, In, and Norwalk, OH.

	Growing Degree Days			
Treatment	**1-May**	**15-May**	**1-October**	**15-October**
		Adrian, MI		
Observed	60	104	1364	1386
MACANoTreatment	(56–76), 68	(110–135), 125	(1437–1508), 1481	(1494–1570), 1531
RCP4.5	(98–142), 118	(174–231), 198	(1708–1954), 1861	(1761–2037), 1930
RCP8.5	(111–187), 144	(196–285), 236	(1901–2241), 2086	(1984–2347), 2190
		Fort Wayne, IN		
Observed	86	148	1615	1648
MACANoTreatment	(77–103), 91	(146–175), 163	(1602–1679), 1650	(1667–1769), 1713
RCP4.5	(132–180), 152	(219–289), 249	(1872–2178), 2046	(1932–2279), 2133
RCP8.5	(140–225), 178	(242–344), 287	(2075–2474), 2279	(2160–2599), 2397
		Norwalk, OH		
Observed	80	129	1493	1516
MACANoTreatment	(58–82), 72	(113–141), 129	(1490–1545), 1515	(1528–1620), 1565
RCP4.5	(109–138), 125	(186–233), 209	(1756–1971), 1894	(1816–2057), 1976
RCP8.5	(126–183), 153	(215–278), 249	(1950–2243), 2115	(2038–2355), 2228

3.4. Basin-Wide Projections

Under medium and high emission scenarios (Table S12) mean precipitation values were expected to remain more or less the same (2.4–3.2 mm) or change only slightly at all stations across the basin, consistent with previous results. Standard deviations were expected to increase, as previously observed, suggesting increases in maximum precipitation. Generally, maximum precipitation was projected to increase across the basin with anticipated increases on average ranging between 35 mm and 130 mm under both RCP 4.5 and RCP 8.5 and values exceeding 600 mm being possible. This was with the exception of Bucyrus, OH and Defiance, OH, for which decreases in maximum precipitation of between 12 mm and 97 mm were predicted by most of the models under both scenarios. Except for Bowling Green, OH and Sandusky, OH, the average maximum dry period length computed from the nine different climate projections was expected to increase compared to the observed data.

Higher daily temperatures could be anticipated under both climate scenarios across the basin (Table S12). Basin-wide, mean maximum temperatures were projected to increase by between 1.5–3.5 °C under RCP 4.5 and 2.5–5.0 °C under RCP 8.5. Absolute maximum temperatures could increase by less than 1 °C in some cases and >10 °C in others when compared to current climatic conditions, potentially putting maximum temperatures at well over 45 °C. Heat stress and heat injury can occur when temperatures rise above 32.2 °C [83,84] and especially if these are sustained. The range of days for optimal growth of corn may decrease if extreme high temperatures persist. Basin-wide, mean minimum temperatures were expected to increase by between 1.3–3.6 °C under RCP 4.5 and 2.1–5.0 °C under RCP 8.5.

4. Discussion

Reliable climate projections are needed to determine hydrologic and water resource responses under different future climate projections with reasonable accuracy and particularly at regional or more localized scales at which actionable policy decisions are made. This can only be achieved if the climate projections for precipitation and air temperature are free from as much bias as possible [15,85]. Biases in climate projections occur mainly because of flawed or faulty ideational boundary assumptions, thus, the use of uncorrected climate projections from downscaled climate models in hydrologic modeling or any other applications can lead to a lot of uncertainty [86–88]. Precipitation estimates are particularly vulnerable to bias, while temperature values can often be used without much correction, if any [50].

Of the two sources of climate projections that were evaluated (GDO and MACA), outputs from MACA were found to be better with or without any treatment to correct the bias. Though the metadata files from the GDO source suggested that the historic period was 1950–2015, this was actually 1950–2005. Very limited information was available in the source documentation, and care must be taken by users to properly understand the historic period before applying future projections to any modeling application. The MACA data used in this study had already been subjected to some bias correction, although such corrections have been found insufficient for treating the bias while downscaling [89]. Thus, in this study, data from the MACA source were further evaluated (precipitation and temperature) and corrected (precipitation only) for bias following which final values were generated for the basin. In this work, it was assumed that gridded downscaled data stayed the same throughout the grid extent and could be compared with the corresponding ground-based station.

The conventional method of bias correction, including power transformation for precipitation outperformed other approaches in this study. Though SWGs have the potential for bias correction due to their ability to preserve the mean and some climate indices, they did not perform well in this study. This poor performance of SWGs was possibly attributable to their inability to compute accurate transitional or conditional probabilities. Thus, the overall efficacy of SWGs in bias correction could be improved if this aspect can be improved.

5. Conclusions

This study suggested that it is important to develop a framework to evaluate and correct bias/error associated with simulated climate output from the most reliable and easy to access statistical downscaled models available in the public domain. With depleting water resources and increasing concern of harmful algae blooms, a reliable future (2006–2099) climate information is needed for use with hydrologic and water resources applications in the WLEB. This would help to determine hydrologic and water resource responses under different future climate projections with reasonable accuracy and particularly at regional or more localized scales at which actionable management decisions are made. The precipitation climate projections require rescaling of the distribution to polarize/unpolarize the impact of extreme precipitation events (both low and high) simulated with bias by regional climate models using boundary conditions. The temperature dataset also requires attention but is well simulated by the climate models. Bias-corrected climate data analysis for WLEB projected a substantial increase in maximum precipitation basin-wide. Temperatures would also be affected at the extremes leading to an overall warmer climate and potential for increases in conditions associated with adverse effects such as heat stress and heat injury. Projected increases in minimum temperatures could, however, result in longer growing seasons, which could be beneficial, although potential benefits could be counteracted by other responses to increasing temperatures such as earlier snowmelt, higher evapotranspiration rates, and heat stress. This study showed that the means and standard deviations are not the only criteria needed to evaluate the performance of downscaling or bias correction methods, rather, other statistical properties and essential characteristics such those related to extremes should also be evaluated. The results from this study were very useful in creating a reliable climate database for the entire WLEB, which can be used in further assessments looking at the impact of changing climatic patterns on water resources in the basin. This study is a step forward in quantifying and correcting the bias in climate (precipitation) projections to support water resource planning and management, an important aspect for hydrologic and water resources studies worldwide.

6. Data Availability

Primary datasets used in this study were obtained from two sources: (1) GDO (authors created acronym for Global Downscaled Climate and Hydrology Projections), available at the URL: https://gdo-dcp.ucllnl.org/downscaled_cmip_projections/; and (2) MACA (Multivariate Adaptive Constructed Analogs), available at the URL: https://climate.northwestknowledge.net/MACA/. Daily summaries of climate data from ground-based climate stations were downloaded from https://www.ncdc.noaa.

gov/cdo-web/datasets. Data generated through this study are published at https://purr.purdue.edu/ [33,34,37,38].

Supplementary Materials: The following are available online at http://www.mdpi.com/2073-4441/11/3/581/s1. Table S1: Statistical properties of daily precipitation (mm) for Adrian, MI; Fort Wayne, IN; and Norwalk, OH from the different climate projection sources in comparison with observed values, Table S2: Performance evaluation in simulating number of wet days in a month by two different climate projection source (GDO and MACA) data for Adrian, MI, Fort Wayne, In, and Norwalk, OH, Table S3: Performance evaluation in simulating number of dry days in a month by two different climate projection source (GDO and MACA) for Adrian, MI, Fort Wayne, In, and Norwalk, OH, Table S4: Extreme event and general climate indices analysis for Adrian, MI; Fort Wayne, IN; and Norwalk, OH from the climate projection sources in comparison with values from observed data, Table S5: Statistical properties of daily maximum air temperature (°C) for Adrian, MI; Fort Wayne, IN; and Norwalk, OH from the climate projection sources in comparison with observed data, Table S6: Statistical properties of daily minimum air temperature, °C, for Adrian, MI; Fort Wayne, IN; and Norwalk, OH from the climate projection sources in comparison with observed data, Table S7: Performance evaluation in simulating Growth Degree Days (GDD) by two different climate projection sources (GDO and MACA) for Adrian, MI, Fort Wayne, IN, and Norwalk, OH, Table S8: Statistical properties of daily precipitation for Adrian, MI, Fort Wayne, IN, and Norwalk, OH based on the different bias correction methods presented on a daily and seasonal basis, Table S9: Statistical properties of daily precipitation, mm, presented on a seasonal basis for Adrian, MI, Fort Wayne, IN, and Norwalk, OH from the MACA climate projections for two different future climate scenarios (RCP 4.5 and RCP 8.5), treated with power transformation bias correction method and original dataset for period from 2006–2099 compared with observed data, Table S10: Extreme event and general climate indices analysis for Adrian, MI; Fort Wayne, IN; and Norwalk, OH from the MACA climate projections for two different future climate scenarios (RCP 4.5 and RCP 8.5), treated with power transformation bias correction method and original dataset for period from 2006–2099 compared with observed data, Table S11: Performance evaluation in simulating number of wet and dry days in a month for Adrian, MI, Fort Wayne, IN, and Norwalk, OH from the MACA climate projections for two different future climate scenarios (RCP 4.5 and RCP 8.5), treated with power transformation bias correction method and original dataset for period from 2006–2099 compared with observed data, Table S12: Details of select statistical properties computed from nine different climate model projections for precipitation (mm) and maximum and minimum temperature (°C) under medium and high emission scenarios (RCP 4.5 and RCP 8.5) for eight different stations in WLEB, Figure S1: (A) (a) Density distribution charts for Fort Wayne, IN for count of monthly precipitation totals, mm, in each year (b) Distribution of annual precipitation totals, mm, with range bound from different climate model outputs. (For the period from 1966–2015 for GDO (right frame) and 1966–2005 for MACA (left frame)); (B) (a) Density distribution charts for Norwalk, OH for count of monthly precipitation totals, mm, in each year (b) Distribution of annual precipitation totals, mm, with range bound from different climate model outputs. (For the period from 1966–2015 for GDO (right frame) and 1966–2005 for MACA (left frame)), Figure S2: (A) Q-Q Plots to evaluate the performance of different bias-correction methods for the period between 1966 and 2005 to reduce the bias in simulating values for daily maximum temperature, °C and present future climate scenarios (2006–2099) for Adrian, MI; (B) Q-Q Plots to evaluate the performance of different bias correction methods for period between 1966 and 2005 to reduce the bias in simulating values for daily maximum temperature, °C and to present the future climatic scenarios (2006–2099) for Fort Wayne, IN; (C) Q-Q Plots to evaluate the performance of different bias correction methods for period between 1966 and 2005 to reduce the bias in simulating values for daily maximum temperature, °C and to present the 48 future climatic scenarios (2006–2099) for Norwalk, OH; (D) Q-Q Plots to evaluate the performance of different bias correction methods for period between 1966 and 2005 to reduce the bias in simulating values for daily minimum temperature, °C and to present the future climatic scenarios (2006–2099) for Adrian, MI; (E) Q-Q Plots to evaluate the performance of different bias correction methods for period between 1966 and 2005 to reduce the bias in simulating values for daily minimum temperature, °C and to present the future climatic scenarios (2006–2099) for Fort Wayne, IN; (F) Q-Q Plots to evaluate the performance of different bias-correction methods for the period between 1966 and 2005 to reduce the bias in simulating values for daily minimum temperature and present future climate scenarios (2006–2099) for Norwalk, OH, Figure S3: (A) Comparison of GDO and MACA climate projection sources for different climate indices for Fort Wayne IN between 1966 and 2005 (GDO_NT: GDO No Treatment; MACA_NT: MACA No Treatment); (B) Comparison of GDO and MACA climate projection sources for different climate indices for Norwalk, OH between 1966 and 2005 (GDO_NT: GDO No Treatment; MACA_NT: MACA No Treatment).

Author Contributions: S.M. designed the study, performed analysis, and wrote the initial drafts of the manuscript under the guidance of M.W.G., who supervised the work and provided guidance for the study design, data analysis, and interpretations. D.C.F., who is the development leader for CLImate GENerator (CLIGEN), provided insights into the results. Both co-authors provided feedback on the writing and contributed to the final manuscript.

Funding: This work was supported in part by the USDA National Institute of Food and Agriculture, Hatch Project 1009404.

Acknowledgments: The authors thank Qi Wang from Statistical Software Consulting, Purdue University for providing insight into R language.

Conflicts of Interest: The authors declare no conflict of interest.

References

1. Obled, C.; Wendling, J.; Beven, K. The sensitivity of hydrological models to spatial rainfall patterns, an evaluation using observed data. *J. Hydrol.* **1994**, *159*, 305–333. [CrossRef]
2. Kouwen, N.; Danard, M.; Bingeman, A.; Luo, W.; Seglenieks, F.R.; Soulis, E.D. Case study, watershed modeling with distributed weather model data. *J. Hydrol. Eng.* **2005**, *10*, 23–38. [CrossRef]
3. Shrestha, R.; Tachikawa, Y.; Takara, K. Performance analysis of different meteorological data and resolutions using MaScOD hydrological model. *Hydrol. Process.* **2004**, *18*, 3169–3187. [CrossRef]
4. Whitehead, P.G.; Wilby, R.L.; Butterfield, D.; Wade, A.J. Impacts of climate change on in-stream nitrogen in a lowland chalk stream, an appraisal of adaptation strategies. *Sci. Total Environ.* **2006**, *365*, 260–273. [CrossRef]
5. Wilby, R.L.; Wigley, T.M.L. Downscaling general circulation model output, a review of methods and limitations. *Prog. Phys. Geogr.* **1997**, *21*, 530–548. [CrossRef]
6. Wilby, R.L.; Wigley, T.M.L. Future changes in the distribution of daily precipitation totals across North America. *Geophys. Res. Lett.* **2002**, *29*, 39-1–39-4. [CrossRef]
7. Wilby, R.L.; Charles, S.P.; Zorita, E.; Timbal, B.; Whetton, P.; Mearns, L.O. Guidelines for Use of Climate Scenarios Developed from Statistical Downscaling Methods. 2004. Available online: http://www.ipcc-data.org/guidelines/dgm_no2_v1_09_2004.pdf (accessed on 12 March 2019).
8. Bosshard, T.; Kotlarski, S.; Zappa, M.; Schär, C. Hydrological climate-impact projections for the Rhine River, GCM-RCM uncertainty and separate temperature and precipitation effects. *J. Hydrometeorol.* **2014**, *15*, 697–713. [CrossRef]
9. Wild, M.; Grieser, J.; Schär, C. Combined surface solar brightening and increasing greenhouse effect support recent intensification of the global land-based hydrological cycle. *Geophys. Res. Lett.* **2008**, *35*. [CrossRef]
10. Winkler, J.A.; Arritt, R.W.; Pryor, S.C. *Climate Projections for the Midwest, Availability, Interpretation and Synthesis*; US National Climate Assessment Midwest Technical Input Report; Great Lakes Integrated Sciences and Assessments Center (GLISA): Ann Arbor, MI, USA, 2012; Available online: http://glisa.msu.edu/docs/NCA/MTIT_Future.pdf (accessed on 19 March 2019).
11. Maurer, E.P.; Brekke, L.; Pruitt, T.; Thrasher, B.; Long, J.; Duffy, P.; Dettinger, M.; Cayan, D.; Arnold, J. An enhanced archive facilitating climate impacts and adaptation analysis. *Bull. Am. Meteorol. Soc.* **2014**, *95*, 1011–1019. [CrossRef]
12. Wang, J.; Kotamarthi, V.R. High-resolution dynamically downscaled projections of precipitation in the mid and late 21st century over North America. *Earth's Future* **2015**, *3*, 268–288. [CrossRef]
13. Teutschbein, C.; Seibert, J. Regional climate models for hydrological impact studies at the catchment scale, a review of recent modeling strategies. *Geogr. Compass* **2010**, *4*, 834–860. [CrossRef]
14. Xu, C. From GCMs to river flow, a review of downscaling methods and hydrologic modelling approaches. *Prog. Phys. Geogr.* **1999**, *23*, 229–249. [CrossRef]
15. Teutschbein, C.; Wetterhall, F.; Seibert, J. Evaluation of different downscaling techniques for hydrological climate-change impact studies at the catchment scale. *Clim. Dyn.* **2011**, *37*, 2087–2105. [CrossRef]
16. Trzaska, S.; Schnarr, E. *A Review of Downscaling Methods for Climate Change Projections*; Produced for the United States Agency for International Development by Tetra Tech ARD; Tetra Tech ARD: Pasadena, CA, USA, 2014; pp. 1–42.
17. Beven, K.J. *Rainfall-Runoff Modelling, the Primer*; John Wiley & Sons: Hoboken, NJ, USA, 2011.
18. Kay, A.L.; Davies, H.N.; Bell, V.A.; Jones, R.G. Comparison of uncertainty sources for climate change impacts, flood frequency in England. *Clim. Chang.* **2009**, *92*, 41–63. [CrossRef]
19. Eden, J.M.; Widmann, M.; Maraun, D.; Vrac, M. Comparison of GCM- and RCM-simulated precipitation following stochastic postprocessing. *J. Geophys. Res. Atmos.* **2014**, *119*, 11040–11053. [CrossRef]
20. Troin, M.; Velázquez, J.A.; Caya, D.; Brissette, F. Comparing statistical post-processing of regional and global climate scenarios for hydrological impacts assessment, a case study of two Canadian catchments. *J. Hydrol.* **2015**, *520*, 268–288. [CrossRef]
21. Ho, C.K.; Stephenson, D.B.; Collins, M.; Ferro, C.A.T.; Brown, S.J. Calibration strategies, a source of additional uncertainty in climate change projections. *Bull. Am. Meteorol. Soc.* **2012**, *93*, 21–26. [CrossRef]
22. Seguí, P.Q.; Ribes, A.; Martin, E.; Habets, F.; Boé, J. Comparison of three downscaling methods in simulating the impact of climate change on the hydrology of Mediterranean basins. *J. Hydrol.* **2010**, *383*, 111–124. [CrossRef]

23. Dobler, C.; Hagemann, S.; Wilby, R.L.; Stötter, J. Quantifying different sources of uncertainty in hydrological projections in an Alpine watershed. *Hydrol. Earth Syst. Sci.* **2012**, *16*, 4343–4360. [CrossRef]
24. Cousino, L.K.; Becker, R.H.; Zmijewski, K.A. Modeling the effects of climate change on water, sediment, and nutrient yields from the Maumee River watershed. *J. Hydrol. Reg. Stud.* **2015**, *4*, 762–775. [CrossRef]
25. Kalcic, M.M.; Kirchhoff, C.; Bosch, N.; Muenich, R.L.; Murray, M.; Griffith Gardner, J.; Scavia, D. Engaging stakeholders to define feasible and desirable agricultural conservation in western Lake Erie watersheds. *Environ. Sci. Technol.* **2016**, *50*, 8135–8145. [CrossRef] [PubMed]
26. Scavia, D.; Kalcic, M.; Muenich, R.L.; Aloysius, N.; Boles, C.; Confessor, R.; DePinto, J.; Gildow, M.; Martin, J.; Read, J. *Informing Lake Erie Agriculture Nutrient Management via Scenario Evaluation*; University of Michigan: Ann Arbor, MI, USA, 2016; Available online: http://tinyurl.com/pp4umuz (accessed on 1 April 2016).
27. Mehan, S.; Guo, T.; Gitau, M.W.; Flanagan, D.C. Comparative study of different stochastic weather generators for long-term climate data simulation. *Climate* **2017**, *5*, 26. [CrossRef]
28. Ficklin, D.L.; Luo, Y.; Luedeling, E.; Zhang, M. Climate change sensitivity assessment of a highly agricultural watershed using SWAT. *J. Hydrol.* **2009**, *374*, 16–29. [CrossRef]
29. Mehan, S.; Kanan, N.; Neupane, R.P.; McDaniel, R.; Kumar, S. Climate change impacts on the hydrological processes of a small agricultural watershed. *Climate* **2016**, *4*, 56. [CrossRef]
30. Abatzoglou, J.T. Development of gridded surface meteorological data for ecological applications and modelling. *Int. J. Climatol.* **2013**, *33*, 121–131. [CrossRef]
31. Brekke, L.; Thrasher, B.L.; Maurer, E.P.; Pruitt, T. *Downscaled CMIP3 and CMIP5 Climate Projections, Release of Downscaled CMIP5 Climate Projections, Comparison with Preceding Information, and Summary of User Needs*; Technical Service Center, Bureau of Reclamation, US Department of the Interior: Denver, CO, USA, 2013.
32. Wood, A.W.; Leung, L.R.; Sridhar, V.; Lettenmaier, D.P. Hydrologic implications of dynamical and statistical approaches to downscaling climate model outputs. *Clim. Chang.* **2014**, *62*, 189–216. [CrossRef]
33. Mehan, S.; Gitau, M. *Climate Projections for the Western Lake Erie Basin for Medium and High Emission Scenarios for Hydrologic Modeling Assessment Studies (Indiana, Ohio, and Michigan)*; Purdue University Research Repository (PURR): West Lafayette, IN, USA, 2019.
34. Mehan, S.; Gitau, M. *Spatial-Temporal Climate Projection Data for 21st-Century for the Western Lake Erie Basin (WLEB) for Hydrologic Studies*; Purdue University Research Repository (PURR): West Lafayette, IN, USA, 2019.
35. Friedlingstein, P.; Meinshausen, M.; Arora, V.K.; Jones, C.D.; Anav, A.; Liddicoat, S.K.; Knutti, R. Uncertainties in CMIP5 climate projections due to carbon cycle feedbacks. *J. Clim.* **2014**, *27*, 511–526. [CrossRef]
36. Sun, Q.; Miao, C.; Duan, Q. Projected changes in temperature and precipitation in ten river basins over China in 21st century. *Int. J. Climatol.* **2015**, *35*, 1125–1141. [CrossRef]
37. Mehan, S.; Gitau, M. *Climate Projection Data for 21st Century for the Western Lake Erie Basin (Indiana, Ohio, and Michigan)*; Purdue University Research Repository (PURR): West Lafayette, IN, USA, 2019.
38. Mehan, S.; Gitau, M. *Climate Time Series Analysis Using R*; Purdue University Research Repository (PURR): West Lafayette, IN, USA, 2019.
39. Lawrence, P.J.; Feddema, J.J.; Bonan, G.B.; Meehl, G.A.; O'Neill, B.C.; Oleson, K.W.; Levis, S.; Lawrence, D.M.; Kluzek, E.; Lindsay, K. Simulating the biogeochemical and biogeophysical impacts of transient land cover change and wood harvest in the Community Climate System Model (CCSM4) from 1850 to 2100. *J. Clim.* **2012**, *25*, 3071–3095. [CrossRef]
40. Palazzoli, I.; Maskey, S.; Uhlenbrook, S.; Nana, E.; Bocchiola, D. Impact of prospective climate change on water resources and crop yields in the Indrawati basin, Nepal. *Agric. Syst.* **2015**, *133*, 143–157. [CrossRef]
41. Straatsma, M.; Droogers, P.; Brandsma, J.; Buytaert, W.; Karssenberg, D.; Van Beek, R.; Wada, Y.; Sutanudjaja, E.; Vitolo, C.; Schmitz, O. Bridging the climate-induced water gap in the twenty-first century, adaptation support based on water supply, demand, adaptation and financing. In Proceedings of the EGU General Assembly Conference Abstracts, EGU General Assembly, Vienna, Austria, 27 April–2 May 2014.
42. Gorguner, M.; Ishida, K.; Kavvas, M.L.; Ohara, N.; Richard Chen, Z.Q. Regional hydrologic impact assessment of climate change on reservoir inflows under the CMIP5 climate projections. In Proceedings of the World Environmental and Water Resources Congress, Sacramento, CA, USA, 21–25 May 2017; pp. 565–571. [CrossRef]
43. Sridhar, V.; Billah, M.M.; Hildreth, J.W. Coupled surface and groundwater hydrological modeling in a changing climate. *Groundwater* **2017**, *56*, 618–635. [CrossRef]
44. Murawski, A.; Bürger, G.; Vorogushyn, S.; Merz, B. Can local climate variability be explained by weather patterns? A multi-station evaluation for the Rhine basin. *Hydrol. Earth Syst. Sci.* **2016**, *20*, 4283–4306. [CrossRef]

45. Song, X.; Hoffman, F.M.; Iversen, C.M.; Yin, Y.; Kumar, J.; Ma, C.; Xu, X. Significant inconsistency of vegetation carbon density in CMIP5 Earth system models against observational data. *J. Geophys. Res. Biogeosci.* **2017**, *122*, 2282–2297. [CrossRef]
46. Peng, S.; Ciais, P.; Krinner, G.; Wang, T.; Gouttevin, I.; McGuire, A.D.; Lawrence, D.; Burke, E.; Chen, X.; Decharme, B. Simulated high-latitude soil thermal dynamics during the past 4 decades. *Cryosphere* **2016**, *10*, 179–192. [CrossRef]
47. Park, Y.S.; Kum, D.H.; Jung, Y.H.; Cho, J.P.; Lim, K.J.; Kim, K.S. Simulation of the Best Management Practice Impacts on Nonpoint Source Pollutant Reduction in Agricultural Area using STEPL WEB Model. *J. Korean Soc. Agric. Eng.* **2014**, *56*, 21–27.
48. Lant, C.; Stoebner, T.J.; Schoof, J.T.; Crabb, B. The effect of climate change on rural land cover patterns in the Central United States. *Clim. Chang.* **2016**, *138*, 585–602. [CrossRef]
49. Ivancic, T. *Towards a Conceptual Understanding of Precipitation and Flooding in a Changing Climate*; State University of New York College of Environmental Science and Forestry: Syracuse, NY, USA, 2016.
50. Knutti, R.; Furrer, R.; Tebaldi, C.; Cermak, J.; Meehl, G.A. Challenges in combining projections from multiple climate models. *J. Clim.* **2010**, *23*, 2739–2758. [CrossRef]
51. Mathugama, S.C.; Peiris, T.S.G. Critical evaluation of dry spell research. *Int. J. Basic Appl. Sci.* **2011**, *6*, 153–160.
52. Sivakumar, M.V.K. Empirical analysis of dry spells for agricultural applications in West Africa. *J. Clim.* **1992**, *5*, 532–539. [CrossRef]
53. Taley, S.M.; Dalvi, V.B. *Dry-Spell Analysis for Studying the Sustainability of Rainfed Agriculture in India—The Case Study of the Vidarbha Region of Maharashtra State*; Large Farm Development Project: Maharashtra, India, 1991.
54. Mathlouthi, M.; Lebdi, F. Characterization of dry spell events in a basin in the North of Tunisia. In Proceedings of the First International Conference on Drought Management: Scientific and Technological Innovations, Zaragoza, Spain, 12–14 June 2008; pp. 43–48.
55. Douguedroit, A. The variations of dry spells in Marseilles from 1865 to 1984. *J. Climatol.* **1987**, *7*, 541–551. [CrossRef]
56. Bai, A.; Zhai, P.; Liu, X. Climatology and trends of wet spells in China. *Theor. Appl. Climatol.* **2007**, *88*, 139–148. [CrossRef]
57. Leander, R.; Buishand, T.A. Resampling of regional climate model output for the simulation of extreme river flows. *J. Hydrol.* **2007**, *332*, 487–496. [CrossRef]
58. Leander, R.; Buishand, T.A.; van den Hurk, B.J.J.M.; de Wit, M.J.M. Estimated changes in flood quantiles of the river Meuse from resampling of regional climate model output. *J. Hydrol.* **2008**, *351*, 331–343. [CrossRef]
59. Chen, J.; Brissette, F.P.; Leconte, R. Uncertainty of downscaling method in quantifying the impact of climate change on hydrology. *J. Hydrol.* **2011**, *401*, 190–202. [CrossRef]
60. Guo, T.; Mehan, S.; Gitau, M.W.; Wang, Q.; Kuczek, T.; Flanagan, D.C. Impact of number of realizations on the suitability of simulated weather data for hydrologic and environmental applications. *Stoch. Environ. Res. Risk Assess.* **2017**, *32*, 2405–2421. [CrossRef]
61. Nicks, A.D.; Lane, L.J.; Gander, G.A. Chapter 2: Weather generator. In *USDA-Water Erosion Prediction Project, Hillslope Profile and Watershed Model Documentation*; NSERL Report #10; National Soil Erosion Research Lab: West Lafayette, IN, USA, 1995.
62. Semenov, M. *LARS-WG 5, A Stochastic Weather Generator for Climate Change Impact Assessments*; Rothamsted Research: Hertfordshire, UK, 2010.
63. Semenov, M.A.; Barrow, E.M. *LARS-WG, A Stochastic Weather Generator for Use in Climate Impact Studies, User Manual*; Rothamsted Research: Hertfordshire, UK, 2002.
64. Auer, A.H., Jr. The rain versus snow threshold temperatures. *Weatherwise* **1974**, *27*, 67. [CrossRef]
65. Lawrence, D.S. *Physical Hydrology*, 3rd ed.; Waveland Press, Inc.: Long Grove, IL, USA, 2015; pp. 203–252.
66. Neild, R.E.; Newman, J.E. *Growing Season Characteristics and Requirements in the Corn Belt*; Cooperative Extension Service, Iowa State University: Ames, IA, USA, 1987.
67. Deni, S.M.; Jemain, A.A.; Ibrahim, K. The spatial distribution of wet and dry spells over Peninsular Malaysia. *Theor. Appl. Climatol.* **2008**, *94*, 163–173. [CrossRef]
68. Pandharinath, N. Markov chain model probability of dry, wet weeks during moonson period over Andhra Pradesh. *Mausam* **1991**, *42*, 393–400.
69. Sonnadara, D.U.J.; Jayewardene, D.R. A Markov chain probability model to describe wet and dry patterns of weather at Colombo. *Theor. Appl. Climatol.* **2015**, *119*, 333–340. [CrossRef]

70. Bhattacharaya, A.K.; Sarkar, T.K. Analysis of rainfall data for Agricultural land drainage design. *J. Agric. Eng.* **1982**, *19*, 15–25.
71. Upadhaya, A.; Singh, S. Estimation of consecutive days maximum rainfall by various methods and their comparison. *Indian J. Soil Conserv.* **1998**, *26*, 1993–2001.
72. Gastwirth, J.L. A general definition of the Lorenz curve. *Econometrica* **1971**, *39*, 1037–1039. [CrossRef]
73. Murphy, A.H. A new vector partition of the probability score. *J. Appl. Meteorol.* **1973**, *12*, 595–600. [CrossRef]
74. Finley, J.P. Tornado predictions. *Am. Meteorol. J.* **1884**, *1*, 85–88.
75. Ferro, C.A.T.; Stephenson, D.B. Extremal dependence indices, Improved verification measures for deterministic forecasts of rare binary events. *Weather Forecast.* **2011**, *26*, 699–713. [CrossRef]
76. Cohen, J. *Statistical Power Analysis for the Behavioral Sciences (Revised Ed.)*; Academic Press: New York, NY, USA, 1977.
77. Cohen, J. *Statistical Power Analysis for the Behavioral Sciences*; Lawrence Earlbaum Associates: Hillsdale, NJ, USA, 1988; pp. 20–26.
78. Glass, G.V.; Smith, M.L.; McGaw, B. *Meta-Analysis in Social Research*; Sage Publications, Incorporated: Thousand Oaks, CA, USA, 1981.
79. Hawkins, E.; Osborne, T.M.; Ho, C.K.; Challinor, A.J. Calibration and bias correction of climate projections for crop modelling, an idealised case study over Europe. *Agric. For. Meteorol.* **2013**, *170*, 19–31. [CrossRef]
80. Fatichi, S.; Ivanov, V.Y.; Caporali, E. Simulation of future climate scenarios with a weather generator. *Adv. Water Resour.* **2011**, *34*, 448–467. [CrossRef]
81. Katz, R.W.; Brown, B.G. Extreme events in a changing climate, variability is more important than averages. *Clim. Chang.* **1992**, *21*, 289–302. [CrossRef]
82. Romero-Lankao, P.; Smith, J.; Davidson, D.; Diffenbaugh, N.; Kinney, P.; Kirshen, P.; Kovacs, P.; Villers Ruiz, L. Part B: Regional Aspects—Contribution of Working Group II to the Fifth Assessment Report of the Intergovernmental Panel on Climate Change. In *Climate Change 2014, Impacts, Adaptation, and Vulnerability*; Barros, V.R., Field, C.B., Dokke, D.J., Mastrandrea, M.D., Mach, K.J., Bilir, T.E., Chatterjee, M., Ebi, K.L., Estrada, Y.O., Genova, R.C., et al., Eds.; Cambridge University Press: Cambridge, UK; New York, NY, USA, 2014.
83. Epstein, Y.; Moran, D.S. Thermal comfort and the heat stress indices. *Ind. Health* **2006**, *44*, 388–398. [CrossRef]
84. Jacklitsch, B.; Williams, W.; Musolin, K.; Coca, A.; Kim, J.; Turner, N. *NIOSH Criteria for a Recommended Standard, Occupational Exposure to Heat and Hot Environments*; NIOSH (National Institute of Occupational Safety and Health): Washington, DC, USA, 2016.
85. Christensen, J.H.; Carter, T.R.; Rummukainen, M.; Amanatidis, G. Evaluating the performance and utility of regional climate models, the PRUDENCE project. *Clim. Chang.* **2007**, *81*, 1–6. [CrossRef]
86. Déqué, M.; Rowell, D.P.; Lüthi, D.; Giorgi, F.; Christensen, J.H.; Rockel, B.; Jacob, D.; Kjellström, E.; De Castro, M.; van den Hurk, B. An intercomparison of regional climate simulations for Europe, assessing uncertainties in model projections. *Clim. Chang.* **2007**, *81*, 53–70. [CrossRef]
87. Kjellström, E.; Nikulin, G.; Hansson, U.L.F.; Strandberg, G.; Ullerstig, A. 21st century changes in the European climate, uncertainties derived from an ensemble of regional climate model simulations. *Tellus A* **2011**, *63*, 24–40. [CrossRef]
88. Mehan, S.; Neupane, R.P.; Kumar, S. Coupling of SUFI 2 and SWAT for improving the simulation of streamflow in an agricultural watershed of South Dakota. *Hydrol. Curr. Res.* **2017**, *8*, 280. [CrossRef]
89. Zhao, T.; Bennett, J.C.; Wang, Q.J.; Schepen, A.; Wood, A.W.; Robertson, D.E.; Ramos, M.H. How suitable is quantile mapping for postprocessing GCM precipitation forecasts? *J. Clim.* **2017**, *30*, 3185–3196. [CrossRef]